BRNO UNIVERSITY OF TECHNOLOGY
VYSOKÉ UČENÍ TECHNICKÉ V BRNĚ

FACULTY OF CHEMISTRY
FAKULTA CHEMICKÁ

INSTITUTE OF PHYSICAL AND APPLIED CHEMISTRY
ÚSTAV FYZIKÁLNÍ A SPOTŘEBNÍ CHEMIE

INFLUENCE OF ANTIBACTERIAL ENZYMES ON PREPARATION AND PROPERTIES OF PHOSPHATE CEMENTS

VLIV PŘÍDAVKU ANTIBAKTERIÁLNÍCH ENZYMŮ NA PŘÍPRAVU A VLASTNOSTI FOSFÁTOVÝCH CEMENTŮ

BACHELOR'S THESIS
BAKALÁŘSKÁ PRÁCE

AUTHOR — Barbora Přečková
AUTOR PRÁCE

SUPERVISOR — Doc. Ing. Lucy Vojtová, Ph.D.
VEDOUCÍ PRÁCE

BRNO 2020

VYSOKÉ UČENÍ TECHNICKÉ V BRNĚ
FAKULTA CHEMICKÁ

Zadání bakalářské práce

Číslo práce:	FCH-BAK1533/2019	Akademický rok:	2019/20
Ústav:	Ústav fyzikální a spotřební chemie		
Studentka:	**Barbora Přečková**		
Studijní program:	Chemie a chemické technologie		
Studijní obor:	Chemie pro medicínské aplikace		
Vedoucí práce:	**doc. Ing. Lucy Vojtová, Ph.D.**		

Název bakalářské práce:

Vliv přídavku antibakteriálních enzymů na přípravu a vlastnosti fosfátových cementů

Zadání bakalářské práce:

1) literární rešerše na téma antibakteriální enzymy (ABE), antibakteriální fosfátové cementy
2) příprava fosfátového cementu s ABE
3) fyzikálně–chemická charakterizace
4) stanovení antibakteriálních vlastností
4) vyhodnocení výsledků
5) závěr

Termín odevzdání bakalářské práce: 31.7.2020:

Bakalářská práce se odevzdává v děkanem stanoveném počtu exemplářů na sekretariát ústavu. Toto zadání je součástí bakalářské práce.

Barbora Přečková student(ka)	doc. Ing. Lucy Vojtová, Ph.D. vedoucí práce	prof. Ing. Miloslav Pekař, CSc. vedoucí ústavu

V Brně dne 31.1.2020

prof. Ing. Martin Weiter, Ph.D.
děkan

ABSTRACT

The subject of the bachelor thesis is to prepare tricalcium phosphate bone cement (CPC) modified with antibacterial enzyme for effective and safe bone infection (osteomyelitis) treatment in comparison to antibiotics therapy. The theoretical part of this bachelor thesis provides informations about the structure of bone, osteomyelitis and treatment of osteomyelitis by different types of antibacterial bone cements, specifically by calcium phosphate bone cements. The experimental part deals with optimization in sample preparation, description of the used methods and characteristics of enzyme release kinetics from the cured CPC. To better understand the enzyme release mechanism from the cement, model both enzyme and protein-loaded CPC samples were also prepared and evaluated. Antibacterial properties of the prepared samples were tested by disk-diffusion, dilution and plate method resulting in the positive inhibition effect of antibacterial enzyme on Gram-positive bacteria (G+) of *Staphylococcus aureus* and methicillin-resistant *Staphylococcus aureus* (MRSA) strains but negligible effect on Gram-negative bacteria (G-) *Escherichia coli.* In the following work, the *in vitro* biocompatibility of the enzyme-loaded cements will be evaluated.

KEYWORDS

Phosphate bone cement, antibacterial enzymes, protein release kinetics, osteomyelitis

ABSTRAKT

Předmětem této bakalářské práce je příprava kostního cementu z fosforečnanu vápenatého modifikovaného antibakteriálním enzymem pro účinnou a bezpečnou léčbu zánětu kosti (osteomyelitidy) v porovnání s léčbou antibiotiky. Teoretická část této bakalářské práce poskytuje informace o struktuře kostí, osteomyelitidě a léčbě osteomyelitidy různými typy antibakteriálních kostních cementů, především cementy na bázi fosforečnanu vápenatého. Experimentální část se zabývá optimalizací při přípravě vzorků, popisem použitých metod a charakteristikou kinetiky uvolňování enzymu z vytvrzeného cementu. Pro lepší pochopení mechanismu uvolňování enzymu z cementu byly připraveny a vyhodnoceny i modelové vzorky fosfátového cementu s enzymy i proteiny. Antibakteriální vlastnosti vzorků byly testovány použitím diskové, diluční a plotnové metody, což vedlo k výsledkům pozitivního inhibičního účinku antibakteriálního enzymu na grampozitivní bakterie (G+) kmenů *Staphylococcus aureus* a methicillin-rezistentní *Staphylococcus aureus* (MRSA), ale zanedbatelnému účinku na gramnegativní bakterii (G-) *Escherichia coli.* V následující práci bude zhodnocena *in vitro* biologická kompabilita cementů obsahující enzym.

KLÍČOVÁ SLOVA

Fosfátový kostní cement, antibakteriální enzymy, kinetika uvolňování proteinů, osteomyelitida

PŘEČKOVÁ, Barbora. *Vliv přídavku antibakteriálních enzymů na přípravu a vlastnosti fosfátových cementů.* Brno: Vysoké učení technické v Brně, Fakulta chemická, 2020. 62 s. Vedoucí bakalářské práce: doc. Ing. Lucy Vojtová, Ph.D.

DECLARATION

I declare that the bachelor thesis has been worked out by myself and that all the quotations from the used literary sources are accurate and complete. The content of the bachelor thesis is the property of the Faculty of Chemistry of Brno University of Technology and all commercial uses are allowed only if approved by both the supervisor and the dean of the Faculty of Chemistry, BUT.

…….

student´s signature

ACKNOWLEDGMENT

I would like to thank deeply to my supervisor doc. Ing. Lucy Vojtová, Ph.D., Ing. Lenka Michlovská, Ph.D., Ing. Kristýna Valová, Ing. Klára Lysáková and to all CEITEC Advanced biomaterials group for their precious advices, professional assistance, kindness and time without which this bachelor thesis would not be such a great experience for me. I would also like to thank to Dr. Edgar B. Montufar (CEITEC BUT) for the preparation of TCP powder, to Ing. Klára Lysáková (CEITEC BUT) for the preparation of PLGA-PEG-PLGA copolymer, to the team of doc. RNDr. Luboš Janda, Ph.D. (VRI Brno) for the preparation of antibacterial enzyme and the possibility of performing antibacterial test, to Ing. Tatiana Fialová (Mendel University Brno) for the possibility of performing antibacterial tests and evaluating the results and to doc. Ing. Klára Částková, Ph.D. (CEITEC BUT) for measuring the particle size of TCP. Nevertheless, I would like to express my gratitude to my family the most for their loving care and support throughout my whole life and studies.

CONTENT

1 INTRODUCTION

Bones are the most important part of a human body. Bones serve as a mechanical support for the body by forming a body construction, provide movement and protect internal organs [1]. Nowadays, the surgical and medical therapy is at a high level, however, medicine still must deal with the post-operative infections after the surgery of bone. The infection can cause major health problems that may not always be well treated. The situation is even worse, because one of the bacteria responsible for these bone infections is methicillin-resistant *Staphylococcus aureus* (MRSA). This widespread pathogen is resistant to almost all currently used antibiotics [2]. In addition, antibiotics can also be harmful to health because of their side effects and toxicity. Therefore, scientists are trying to find new materials that would ship an antimicrobial agent directly to the place of the infection and thus support bone regeneration [3]. In addition to antibiotics, there are many other substances showing antibacterial properties, for example nanoparticles, antibacterial enzymes or peptides, bacteriophages, natural herbal extracts etc.

Calcium phosphate cement (CPC) is one of those materials having many advantages over other bone substitutes. CPC has great properties because it is biocompatible, bioactive, osteoconductive and biodegradable substitute and chemically it is similar to mineral part of human bone. Moreover, CPC injectability allows the cement to be used in a mini-invasive surgery and perfectly fit into the site of the bone defect. CPC setting reaction takes place at 37 °C making the material suitable as a carrier for drugs or biological molecules without damaging surrounding environment [2][4]. CPCs have a wide range of utilization in orthopaedics, traumatology and stomatology [5].

Lysostaphin is one of the antibacterial agents with big potential to fight against Gram-positive bacteria. It is an antibacterial enzyme belonging to bacteriocins produced by staphylococci and they may be active against their related bacterial strains [6].

The goal of this bachelor thesis is to prepare antibacterial CPC releasing lysostaphin to potentially treat bone infections as a replacement for antibiotic therapy.

2 THEORETICAL PART

2.1 Bone Infection

The major structure of a human body is made up of the skeleton, which includes 213 bones. The skeleton has many functions as a mechanical support for all body, protection of inter organs, movement and storage of minerals and growth factors [1].

Bone serves as a connective tissue which contains four cell types: osteocytes, osteoclasts, osteoblasts, and bone lining cells [7]. The skeleton can be also divided into two groups of bone, cortical (compact) and trabecular (spongy). The cortical bone makes a hard-exterior cover around bone marrow containing blood vessels. The trabecular bone serves for filling of the centre of the long bones, flat bones and vertebrae. The all outer surface of bone is covered by periosteum, which major function is in growth and fracture repair (see Figure 1) [1][8]. There are four major categories of bones [1]:

- **Long bones** – including the femurs, radii, tibiae
- **Short bones** – including the carpal and tarsal bone
- **Flat bones** – including the skull, scapulae, ribs
- **Irregular bones** – including the vertebrae, sacrum

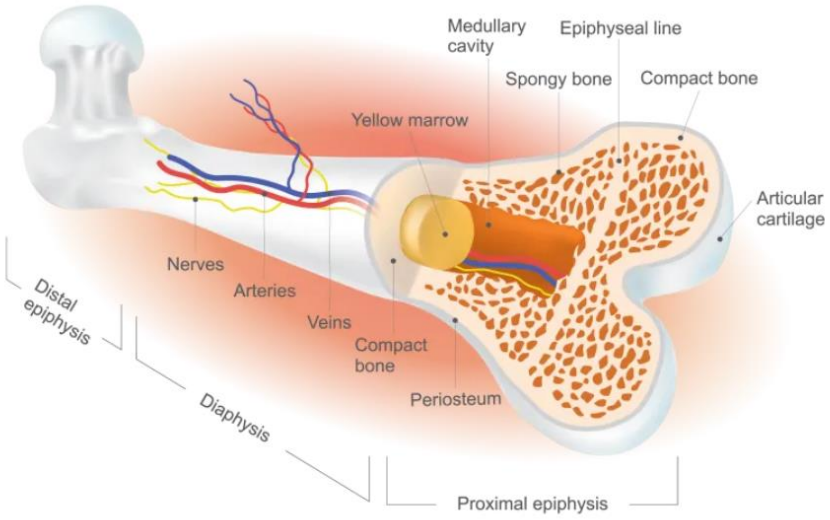

Figure 1: Structure of the femoral bone [9].

One of the post-operative threats associated with bones, which we want to prevent is the development of an infection. Bone inflammation means osteomyelitis in other words. About 10-100 per 100 000 humans fight with osteomyelitis every year [10].

There are two processes causing osteomyelitis: **haematogenous** and **contiguous**. The haematogenous happens when an infection is transmitted by blood system while the contiguous is caused by a pathogen entering the bone in an open fracture during an operation or inserting some foreign implants. This disease is presented by pain, fever, reduced mobility and swelling for a longer time while infected and necrotic tissue is formed. Its consequences can be life-threatening, so a medical help is required (Figure 2) [11]. Unfortunately, increasing

numbers of orthopaedic surgeries bring many serious complications regarding infections, failures of implants, that lead to higher morbidity and mortality rates [12].

Figure 2: Pre-operative photo showing infected left fibula of 65-year-male patient. The injury was presented by edema, redness, sinuses and dilated veins of left leg. The osteomyelitis was caused by a screw implant inserted 10 years back after tibial plateau fracture (a). The second photo shows necrotic tissue being removed during operation (b) [13].

2.1.1 Causative Organisms

Staphylococcus aureus is coagulase-positive staphylococci bacteria (CoPS). This widespread pathogen is responsible for many serious infections, including osteomyelitis, caused by production of toxins, occurring also in hospitals on doctor's tools covered by staphylococcal biofilms [11].

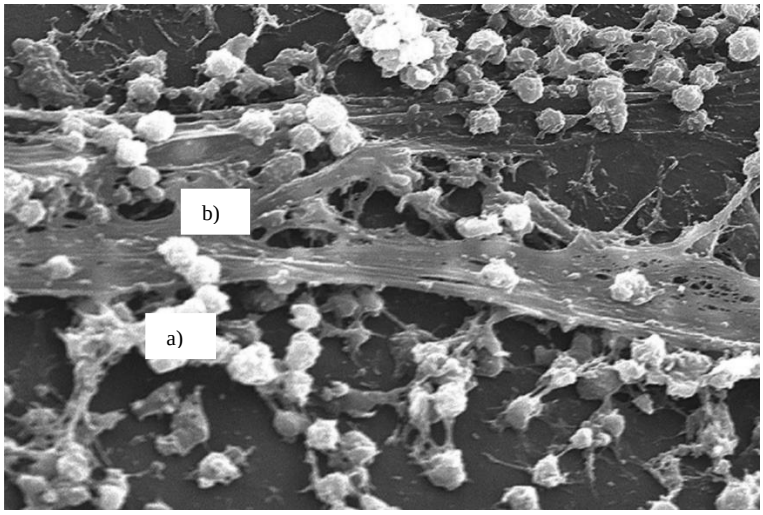

Figure 3: Staphylococcus aureus biofilm, where a) are groups of bacteria in b) an extracellular matrix [10].

Figure 3 shows the biofilm of *Staphylococcus aureus*, which structure is formed by bacteria (a) and extracellular matrix (b) containing DNA, proteins and cell polysaccharides. The biofilm protects the bacteria against antibiotics and makes it easier to adhere to a surface [10]. The most frequent infections appear after an implantation of medical devices into human body, in open wounds as burns and many more [11].

2.1.2 Staphylococcal Resistance

The staphylococcal resistance to nearly all prescribed antibiotics is being a huge problem [14]. Therefore, doctors usually use very active vancomycin for the treatment of infections induced by methicillin-resistant *Staphylococcus aureus* (MRSA). The methicillin resistance is controlled by *mecA* or *mecC* gene which is placed on chromosomal cassette of staphylococcal pathogens. The gene is responsible for encoding penicillin that is bound by PBP2A or PBP2ALGA proteins. They crosslink the peptidoglycans in cell wall of bacteria. These proteins' low affection for β-lactams leads to multidrug resistance of staphylococcal pathogens [14]. Unfortunately, some of the strains of MRSA are also less susceptible to vancomycin, which means that doctors can not always rely on this drug. There is an urgent need for future search and development of new antimicrobial agents after considering all previous facts [14]. Summary of causative organisms and their risk factors in bone and joint infections are described in Table 1.

Table 1: Summary of causative organisms and their risk factors in bone and joint infections [10].

Disease	Causative organisms	Diagnostic clues
Osteomyelitis	*Staphylococcus aureus* (90% adults, >50% children)	Bacteraemia, soft tissue infection
	Streptococcus pyogenes (group A)	Skin infection, trauma
	Streptococcus groups C and G	Diabetes mellitus, immonocompromise
	Group B *Streptococcus*	Neonate, elderly patient
	Gram-negative bacilli (e.g. *Escherichia coli*, *Salmonella*)	Sickle cell disease
	Polymicrobial (5%)	Post-traumatic
	Mycobacterium tuberculosis	Geographical association; more common with immunocopromise; vertebral disease especially
	Brucella spp	Exposure to infected animals or milk; typically vertebral bodies and long bones; classically indolent presentation
	Fungi	Immunocompromised host; post-traumatic
	Haemophilus influenzae	Paediatric patients; very uncommon since introduction of Hib vaccine
	Kingella kingae	Children <3 years of age; may require specialized diagnostic methods
	Bartonella henselae	Exposure to cats; vertebral and limb girdle infection
Septic arthritis	*Staphylococcus aureus*	Bacteraemia; cellulitis around joint
	β-Haemolytic streptococci	Bacteraemia; cellulitis
	Streptococcus pneumoniae	May be multiple joints; associated with better functional outcome than other pathogens
	Neisseria gonorrhoeae	Often multiple joints; young, sexually active adults; also neonates
Prosthetic joint infection	*Staphylococcus aureus*, β-haemolytic streptococci, enterococci	Inoculated at time of operation; strong association with surgical site infection
	Coagulase-negative staphylococci, *Propionobacterium acnes*	Low pathogenicity, biofilm-forming organisms; indolent presentation
	Staphylococcus aureus, Gram-negative bacilli	Haematogenous seeding from infection elsewhere

2.2 Treatment of Bone Infection

When fighting bone infections, it is first important to understand and be aware of what is going on biologically during the infection. Then it is possible to find ways to prevent such illnesses and to start their treatment. This chapter provides information about methods applied in osteomyelitis althoug they have been used on a market for a long time or they bring us a new future perspective [3].

2.2.1 Oral Dosing via Antibiotics

Antibiotics play a very important role in combating infections and related diseases. The discovery of antibiotics is attributed to Alexander Fleming in 1928, but the rocket growth in the production of penicillin started in 1941. Since then, hundreds of antibiotics have been identified and have been used in many cases dealing with infections. They can cause either bacteriostatic or bactericidal effects [16].

Mechanism of Antibiotic Action

Antibiotics are classified on the basis of their mechanism of action (Figure 4) [16]:

- Inhibiting synthesis of bacterial cell walls (penicillins)
- Interfering with microorganism's cell membrane (polymyxins)
- Inhibiting synthesis of proteins – 30 S and 50 S ribosomal subunits (tetracyclines)
- Affecting major metabolic processes of microorganisms (sulphonamides)

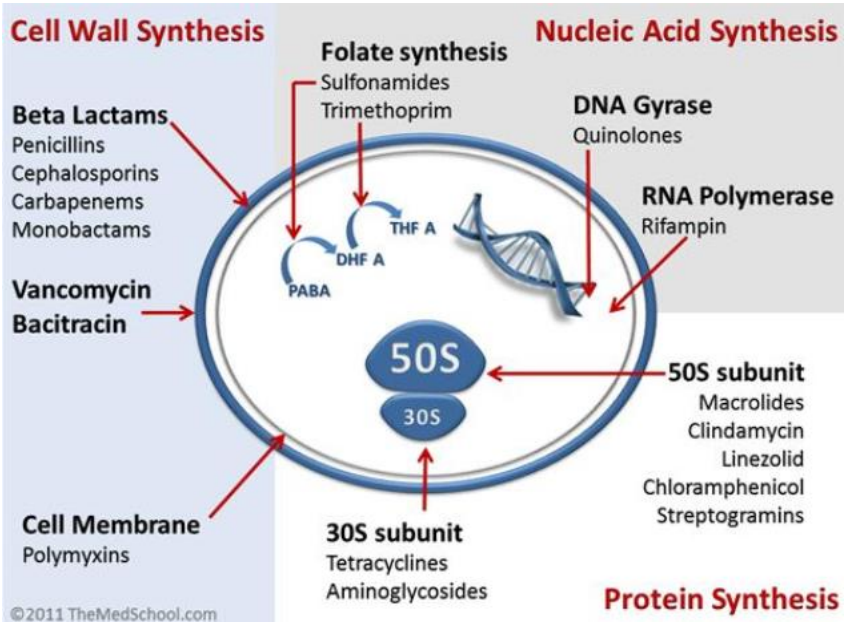

Figure 4: Mechanism of action of antibiotics [17].

Unfortunately, there are also huge disadvantages in using antibiotics such as side effects [16]. Some antibiotics, even effective, have shown to be toxic in other tissues or organs of the body. This huge problem has an urgent need to find a way to deliver the antibiotics directly to the site of infection and to avoid toxicity.

The most traditional way of delivering antibiotics to a human body is through oral intake but with this comes the above-mentioned problem of cytotoxicity and allergic reactions in other body parts. Oral therapy is usually advised after intravenous therapy after a revision surgery for many weeks [18]. There are many antibiotics given orally as: ciprofloxacin, enoxacin, linezolid, fusidic acid, rifampin in combination with other antibiotics, clindamycin, ofloxacin and others [19].

2.2.2 Antimicrobial Bone Cements

Researchers are trying to find new and successful methods and materials to distribute antimicrobial agents to the site of infection, to release the agent effectively and to support bone regeneration and growth by addition of these materials [3]. A suitable solution seems to be antimicrobial agent-loaded bone cements. Charnley [20] developed the first bone cement in the 1960s using poly (methyl methacrylate) (PMMA), which remains the most widely used material for fixation of orthopaedic joint replacements. The discovery of bioactive ceramics from the calcium-phosphate system resulted in the development of new cements. These investigations ranged from the development of castable bioactive materials to modified bioactive composites [20].

2.2.2.1 *Poly (methyl methacrylate) Bone Cement*

Poly (methyl methacrylate) (PMMA) is a representative of bone cement with a quite long history. PMMA is an acrylic polymer composed of two parts, which are MMA monomer and MMA-styrene copolymer [22]. There comes a polymerization reaction while mixing these two components which leads to formation of a cured PMMA. The polymerization reaction is an exothermic process leading to the release of heat. The temperature during curing can reach up to 110°C, which can cause tissue necrosis and bone damage. Another disadvantage of PMMA cements is that they are not absorbable and they do not ensure the new bone growth [23][24].

One of the widely used antibiotic additive in PMMA cements is gentamycin sulphate. Gentamycin belongs to aminoglyside antibiotics inbihiting protein synthesis. It is a heat stable antibiotic dealing well with high temperatures while setting of the cement. Commercial PMMA cements are usually loaded by 0.5-1 g of gentamycin sulphate per 40 g of cement. This addition can be responsible for significant reductions of mechanical properties such as strength. Another drawback is poor dispersion of powdered antibiotic in the cement, which results in an uncontrolled release of a small amout of incorporated gentamycin [25].

2.2.2.2 *Calcium Sulphate Bone Cement*

Another type of bone cement being used in orthopaedics for a long time is **calcium sulphate** [26]**.** It is also osteoconductive, bioresorbable and easily injectable material stimulating new bone growth. One of its disadvantages is that its resorption rate while in vivo using is faster than the rate of new bone creation, which causes the formation of immature bone in the bone defect. Calcium sulphate is usually prepared in two forms: paste or pellets [23][27].

One of the commercially available representatives of calcium sulphate cement is Osteoset®(Wright). There also exists Osteoset®-T (Wright), which is a medical-grade α-hemihydrate calcium sulphate loaded by tobramycin. It consists of small pellets having 4.8 mm in diameter and 3.3 mm in length. Tobramycin is a water-soluble aminoglycoside antibiotic which has a similar bactericidal action like gentamicin. It is effective against both Gram-negative and Gram-positive bacteria [27]. Figure 5 shows the usage of Osteoset®-T as a bone graft substitute in the treatment of chronic osteomyelitis of the tibia. The results proved to be positive after operation of 57-year-old man with post traumatic chronic tibial osteomyelitis [29].

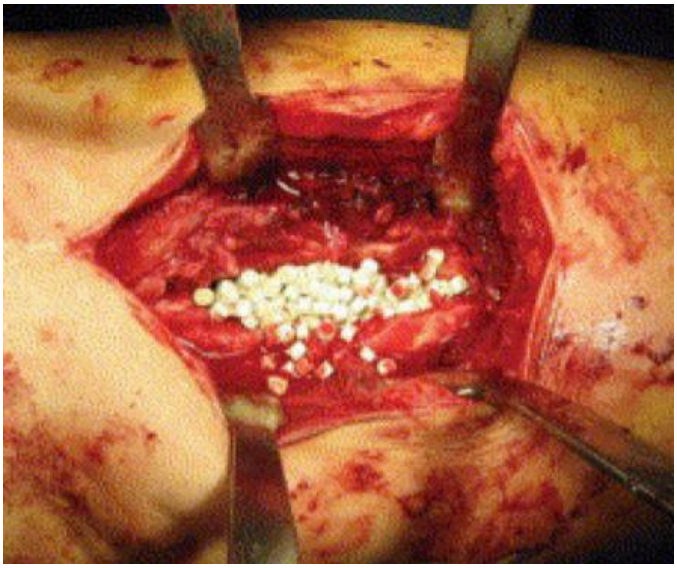

Figure 5: Intra-operative use of Osteoset-T pellets [29].

2.2.2.3 *Calcium Phosphate Bone Cement*

One of the most popular materials used in this problematic is **calcium phosphate**. They can be drug loaded and they promote bone compatibility mostly due to the fact it is a natural component of bone [3]. Calcium phosphate cements are self-setting and self-hardening cements. Their major feature is injectability and paste consistency so they can fit into different spaces of bone and contour defects [4]. Calcium phosphate cement (CPC) is a mouldable paste which is widely used for bone treatment [30]. CPC is chemically similar to mineral part of human's bone which is very advantageous over other types of cements [4].

There are two types of calcium phosphate cements: apatite and brushite. The apatite cements are represented by hydroxyapatite and calcium-deficient hydroxyapatite and the brushite by dicalcium phosphate dihydrate. The production of the cement starts by a mixture of a powder

part (α-TCP, β-TCP…) with a liquid phase, most often pure water or physiological saline [4][30]. Then the powder dissolves and new crystals are formed by precipitation. The crystals grow and entangle to each other, so the CPC becomes a mechanical, stable and hardened solid phase material [4].

Tricalcium Phosphate

The chemical formula is $Ca_3(PO_4)_2$. Tricalcium phosphate has three representative forms depending on the temperature phase conversion:

- **α-TCP** (monoclinic)
- **β-TCP** (rhombohedral)
- **α'-TCP** (hexagonal)

The phase conversion of these three types was described in the Kreidler and Hummel's phase diagram. The β-TCP transforms to α-TCP by healing at 1125 °C and next healing at 1430 °C will lead to transformation to α'-TCP. The hexagonal phosphate only lasts above this high temperature, otherwise it immediately returns to its original form (Figure 6) [31].

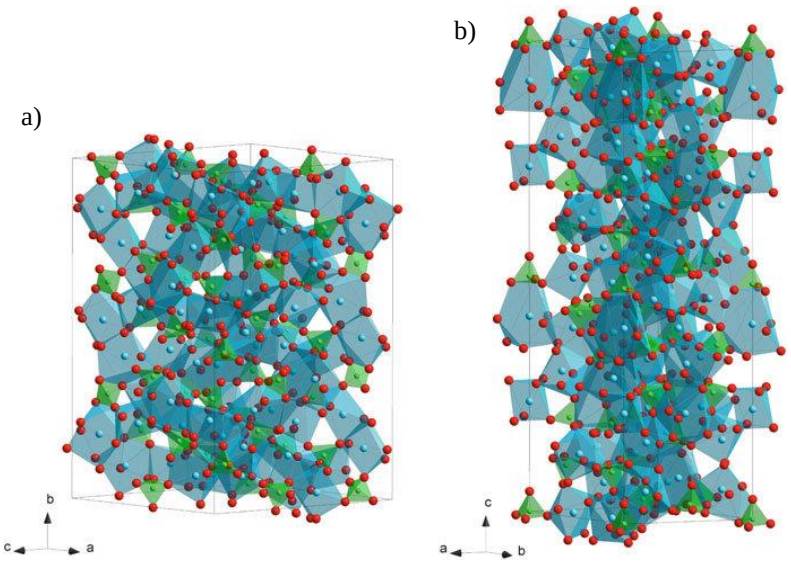

Figure 6: Crystal structures of α-TCP (a) and β-TCP (b) [32].

α-TCP has proven to be an interesting part in production of CPCs mostly thanks to its good solubility. α-TCP is chemically almost the same as β-TCP, but they differ in crystalline structure, which is responsible for lower solubility of β-TCP [33]. The solubility is a major property that is highly related to calcium (Ca)/phosphorous (P) ratio. The Table 2 describes some calcium phosphate's ratios [33].

Mixing a liquid and the α-TCP powder creates a very hardened product, which utilization is popular in bone healing or connecting another required material with bone tissue. α-TCP is hydrolytically transformed into calcium deficient hydroxyapatite after contact with water, which generates the cement to be even more biocompatible. The reaction is showed in the following Equation [35].

$$3\ \alpha\text{-}Ca_3(PO_4)_2 + H_2O \rightarrow Ca_9(PO_4)_5(HPO_4)OH \quad (1)$$

Table 2: The calcium phosphates arranged according to calcium (Ca) and phosphorus (P) ratio [33].

Name	Abbreviation	Formula	Ca/P ratio
Monocalcium phosphate monohydrate	MCPM	$Ca(H_2PO_4)_2.H_2O$	0.5
Dicalcium phosphate anhydrate (monetite)	DCPA	$CaHPO_4$	1.0
Dicalcium phosphate dihydrate (brushite)	DCPD	$CaHPO_4.2H_2O$	1.0
Octacalcium phosphate	OCP	$Ca_8H_2(PO_4)_6.5H_2O$	1.33
β-Tricalcium phosphate	β-TCP	$Ca_3(PO_4)_2$	1.5
Amorphous calcium phosphate	ACP	$Ca_3(PO_4)_2.nH_2O$	1.5
α-Tricalcium phosphate	α-TCP	$\alpha\text{-}Ca_3(PO_4)_2$	1.5
Hydroxyapatite	HA	$Ca_{10}(PO_4)_6(OH)_2$	1.67
Tetracalcium phosphate	TetCP	$Ca_4(PO_4)_2O$	2.0

Usage of Calcium Phosphate Cements

CPCs can cure and harden under physiological conditions due to their self-setting feature [30]. The main advantage of CPCs is their high moldability, osteoconductivity and biocompability as was mentioned before [36]. These three properties ensure that implanted cement is not toxic to the surrounding environment of body, because the end products (apatite and brushite) are biocompatible after dissolution-precipitation reactions. Furthermore, this biomaterial serves as a scaffold and constructs new bone formation [37]. One of the important characteristics is their injectability, which allows them to be implanted quickly during mini-invasive surgical procedures so we can avoid large scars and painful recovery after a surgery [30][37]. Their potential lies in traumatology, stomatology and orthopaedics helping with fractures, fixing implants, or repairing bone defects as they are replacement biomedical materials. They should not only stimulate bone healing, but also provide adequate defensive mechanism against bacterial infections by adding an antibacterial component [5].

One of the commercially available calcium phosphate cements is Norian SRS® (Synthes), which is injectable, osteoconductive and bioresorbable [23]. For example, the Norian calcium phosphate cement was used in corrective osteotomies of the distal radius in the elderly to fix input implant as shown in the following Figure 7 [38].

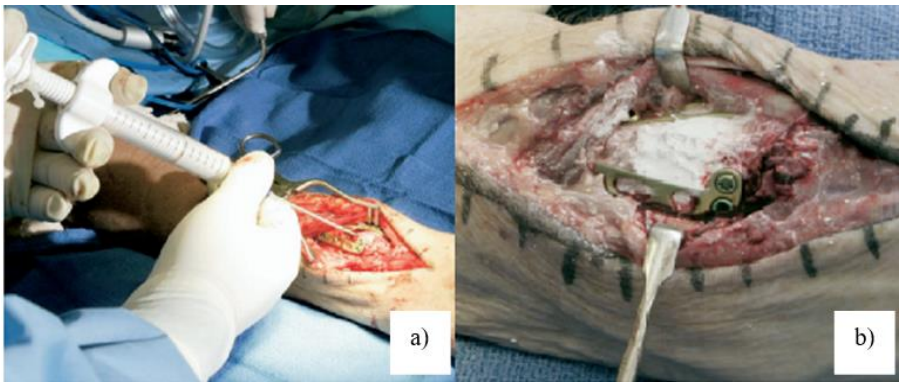

Figure 7: Filling the defect by injectable Norian cement (A), final result after fixing the implants and filling the defect with Norian cement [38].

Antibiotic-loaded CPC

CPCs can serve as carriers for antibiotics for their local release. The drug is dispersed throughout the whole volume of the CPC by adding it into the liquid or the solid phase of the cement, which enable releasing the drug over a longer time. Generally, CPCs are the diffusion controlled devices, where the drug diffuses through the cement matrix. The drug release is influenced by many factors such as the microstructure, the bond between the drug and the matrix or the drug's solubility. As a result of adding a drug into CPCs, there can be changes in the setting reaction rates or in mechanical properties such as strength of the cements [39].

Vancomycin

Nowadays, there are many antibiotics being commonly used and effective in the osteomyelitis treatment as: vancomycin, penicillin, clindamycin, metronidazole, doxycykline and others [39]. Vancomycin is one of the first-line drugs dealing with MRSA infections as it is active against Gram-positive bacteria. It is also used for patient who are allergic to penicillins or cephalosporins. This antibiotic is considered to be one of the oldest and it has been used for decades in the treatment of osteomyelitis. However, there are isolates of *Staphylococcus aureus* being less susceptible to vancomycin. The problem could be in slow bactericidal action. The isolates are decribed as vancomycin-susceptible *S. aureus* (VSSA), vancomycin-intermediate *S. aureus* (VISA) and vancomycin-resistant *S. aureus* (VRSA). If vancomycin does not achieve positive results, the therapy should switch into using an alternative drug, usually daptomycin [14][40].

In a study by Chen et al. [41], calcium phosphate cements with different doses of vancomycin were prepared. The ratios of vancomycin weight to CPC weight were as 0%, 5%, 10%, 15%, 20%, 25% and 30%. They tested antimicrobial activity of vancomycin against MRSA (ATCC 6835), which contaminated blood agar plate. The best results appeared with 5% and 10% vancomycin groups whose O-rings were visible at all time points while 20% and 30% samples proved no inhibition after 8 weeks. The 5% and 10% vancomycin samples inhibited the growth of *S. aureus* for at least 8 weeks, which is very advantageous in the treatment time of osteomyelitis. They also studied the compressive strength of the vancomycin-loaded CPC on a testing machine. The highest compressive strength value exhibited the sample without the addition of vancomycin (0%). The higher the ratio of vancomycin/CPC was, the lower was the compressive strength of the CPC.

Nanoparticles-loaded CPC

Nanoparticles are another antibacterial agent with promising and beneficial effects. There are many currently used nanoparticles as silver, zinc, copper, selenium, and others. Each type of nanoparticle varies in size, shape and in surface curvature, which is critical for final antibacterial activity and mechanism. Their usage is very wide in medical applications. They can serve as antibacterial coating of implanted devices, such as dental implants or cardiovascular apparatuses. For example, titanium oxide is being applied for inhibiting the adhesion and growth of bacteria. Another great result appears in bone cements mixed with silver nanoparticles (AgNPs) defending the surface biofilms formation [43][44].

Mechanism of Nanoparticles Action

Nanoparticles must be in contact with the bacterial cell to have antibacterial functions. The contact is provided by Van der Waals forces, hydrophobic interactions, and electrostatic forces. Nanoparticles then enter the bacteria through its membrane to change the bacterial metabolic system, influence their shape and disable the cell membrane. Nanoparticles also search for interactions with cell's components as DNA, enzymes, and ribosomes to deactivate proteins, change the cell membrane permeability, inhibit enzymes and disbalance electrolyte standards (Figure 8) [44].

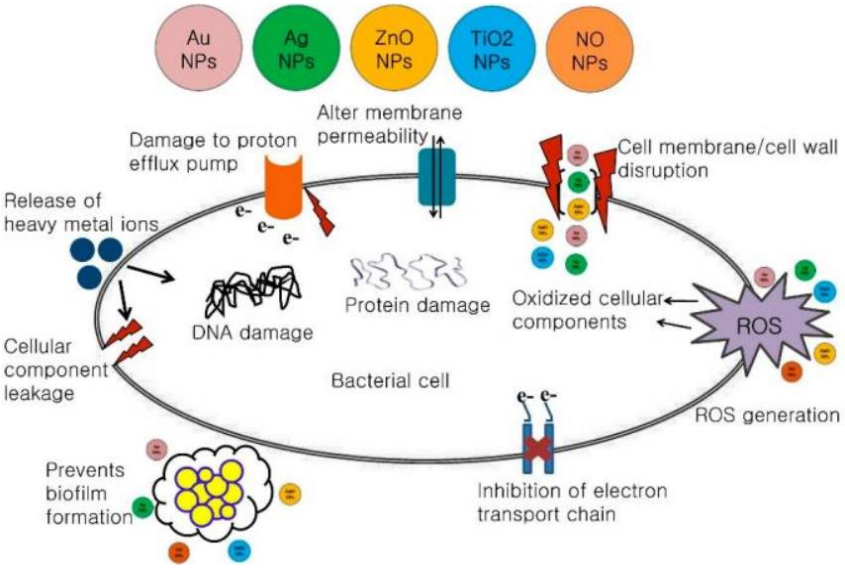

Figure 8: Antimicrobial mechanism of different types of nanoparticles [45].

Selenium is one of the nanoparticles with high potential to be used in biomaterials. Selenium is found naturally in the human body and it has many health benefits as anti-cancer function, brain function, bone tissue function, anti-heart disease function and others. It has been proven that selenium is very important for the right function of bone tissue. Selenium absences could slow down the bone growth and effect the metabolism of bone tissue [45]. Selenium nanoparticles (SeNPs) proved to have antibacterial activity against *Staphylococcus aureus* and *Pseudomonas aeruginosa* in hydroxyapatite coatings. The selenium-coated material inhibited the formed biofilms of bacteria even at concentration of 0,6% weight of selenium

in the coating [47]. SeNPs-loaded CPC has been studied in the diploma thesis by Grézlová (CEITEC BUT) [48]. SeNPs exhibited first-order release kinetics within first day from CPC with antibacterial efficacy value of about 10 ppm.

Antimicrobial Peptides-loaded CPC

Antimicrobial peptides (AMPs) are everywhere in the nature and they are a part of the first defence lines of organisms against infectious microorganisms [49]. They are capable of rapidly and efficiently killing pathogenic microorganisms such as bacteria, yeast, or viruses. AMPs are made from five to over hundreds of amino acids. The first notes and discovery of AMPs date back to 1939, when an extract of *Bacillus* tribe was gained from soil. In following years, other perspective AMPs were found. There are about five thousand of known AMPs (natural or synthesized) over the years of research. Both prokaryotes (bacteria…) and eukaryotes (animals, plants, fungi…) are a potential source of natural AMPs. Most of AMPs expose hydrophilic and hydrophobic character as they are amphiphilic molecules [50]. AMPs can be classified into four groups (Figure 9) [49]:

a) β-leaf structure
b) α-helical structure
c) loosened peptide
d) peptide loop

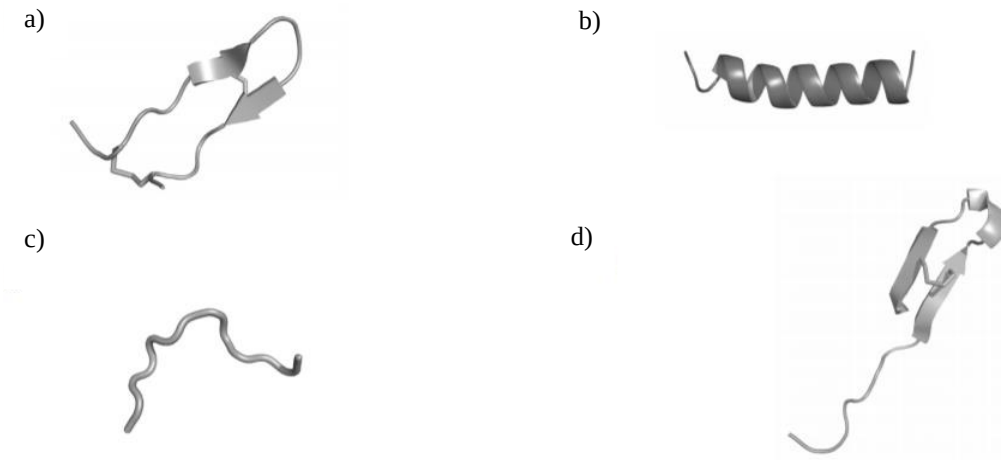

Figure 9: General structures of AMPs [49].

Mechanism of Antimicrobial Peptides Action

Microorganism cell membrane is made up of phospholipids that are negative charged. Most studied AMPs are the cationic ones. The mechanism consists in electrostatic interactions between the cationic peptide and the outer negative charged bacterial membrane containing anionic lipids [50]. A repulsion of cations Ca^{2+} and Mg^{2+} destabilizes the membrane so the peptide can approach the cytoplasm and destruct proteins followed by DNA and RNA [49]. We can name those peptides as membrane active [50].

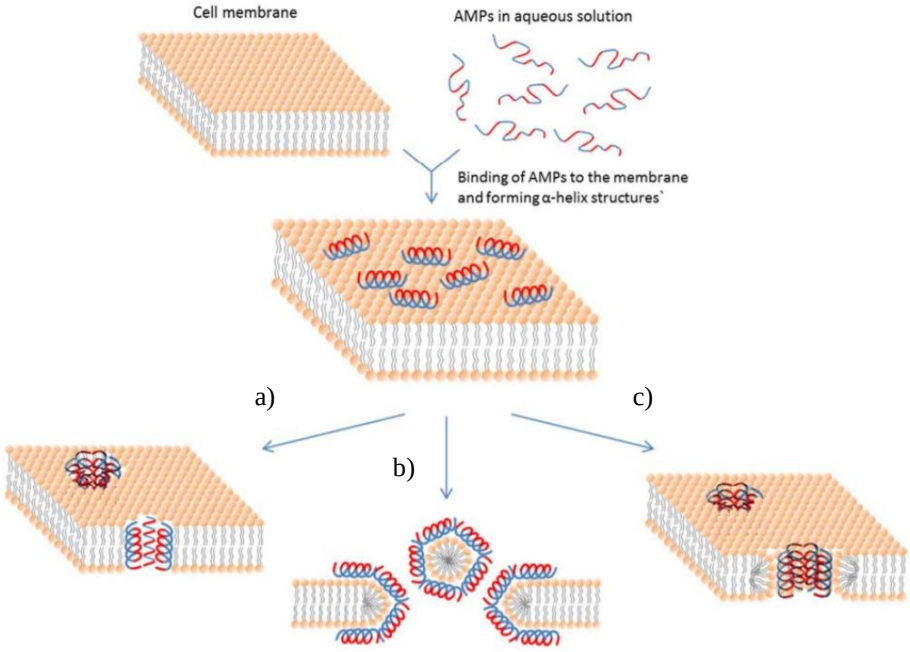

Figure 10: Schematic representation of some action mechanisms of membrane active AMPs [50].

The Figure 10 shows the AMPs mechanism of action on cell membranes in three ways [47]. The hydrophilic part of AMP is red coloured, while the hydrophobic is pictured blue.

a) Barrel-Stave model. AMP molecules attack the membrane in a perpendicular direction.
b) Carpet model. AMP surrounds a small area of the membrane by its hydrophobic part.
c) Toroidal pore model. This model is similar with the first one **(a),** but AMPs have connections with the main phospholipid membrane parts.

There are many works and research proving great results in application of AMPs against bacterial cells creating such dangerous biofilms [50]. In a study by Stallmann and colleagues [51], they examined antimicrobial activity of hLF1-11 peptide which is human lactoferrin usually found in human milk, tears, saliva, nasal and bronchial mucosa [52]. They used different calcium phosphate cements to serve as carrier matrix for this peptide. The results appeared to be successful when hLF1-11 significantly reduced MRSA infection.

Enzybiotics-loaded CPC

‘‘Enzyme’’ and ‘‘antibiotic’’ are two words terming the enzybiotics. They are presented by lytic enzymes that can be found in nature in bacteria, viruses also in body fluids as mucous, tears and others. These enzymes target the cell walls of Gram-positive bacteria and cause their complete demolish. Enzymes show their selectivity without interfering with microflora. One of the most studied enzymes are peptidoglycan hydrolases containing two domain structures [53]:

- **N-terminal catalytic domain** serving for cell wall disruption
- **C-terminal domain** responsible for peptidoglycan binding.

Peptidoglycan hydrolases including following enzymes are [53]:

- **Lysins**
- **Endolysins**
- **Autolysins**
- **Lysozymes**
- **Bacteriocins**

Only selected enzymes closely related to the proposed work are described below.

Lysozyme

Lysozyme belongs to one of the important enzymes and is naturally present in plants, bacteria, mammals and birds. It can be found in a wide variety of fluids such as breast milk, tears and saliva secretions. Lysozyme molecular weight is about 14.4 kDa. One of the major properties of lysozyme is its antimicrobial activity against a wide range of bacteria and fungus. Lysozyme can hydrolyze the β(1-4) glycosidic bonds between *N*-acetylmuramic acid and *N*- acetylglucosamine, which leads to the destruction of the bacterial cell wall. This glycosidase enzyme is more effective against Gram-positive bacteria than Gram-negative bacteria because Gram-negative bacteria have one more outer membrane. [53][55].

The Figure 11 illustrates the differences in the structure of Gram-positive and Gram-negative bacteria. Two key features which lead to the differing visualization properties of Gram-positive and Gram-negative species are the thickness of the peptidoglycan layer and presence or absence of the outer lipid membrane. This is because the wall structure affects the cell’s ability to retain the crystal violet stain used in the Gram staining procedure which can then be visualized under a light microscope. Gram-positive bacteria have a thick peptidoglycan layer and no outer lipid membrane whilst Gram-negative bacteria have a thin peptidoglycan layer and have an outer lipid membrane [56].

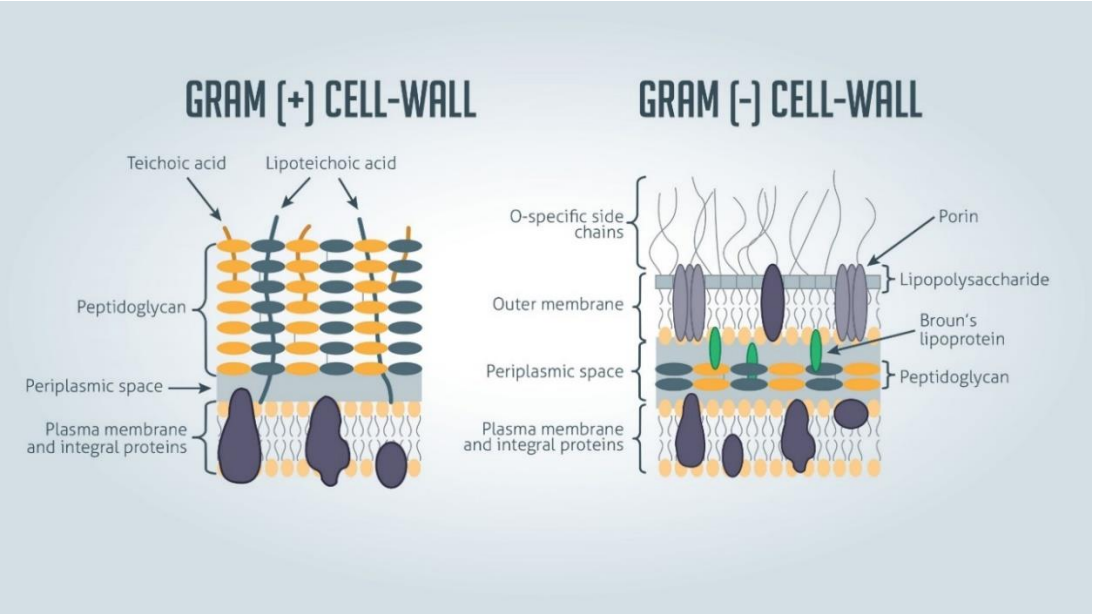

Figure 11: Difference in structure of Gram-positive vs Gram-negative bacteria [56].

Lysostaphin

Lysostaphin is known as the Class III bacteriocin which present large and heat-labile proteins. Bacteriocins are antimicrobial compounds and they belong to peptidoglycan hydrolases. These are proteins or peptides derived from bacteria that can be effective on similar or related bacterial strains by bactericidal or bacteriostatic impact. It is clear, that almost all bacterial strains are responsible for production of at least one bacteriocin. BACTIBASE is a present database consisting of about 219 notes describing proteins or peptides from Gram-negative and Gram-positive bacteria. One of the well-studied bacteriocins is lysostaphin [57].

Mechanism of Lysostaphin Action

Lysostaphin belongs to a class called staphylococcins, that are products of staphylococci [6]. Its molecular weight is approximetely 25 kDa [57]. It is a bacteriolytic enzyme able of lysing peptidoglycan placed in a bacterial cell wall. The peptidoglycan plays a major role in strength and growth of the cell shape and defends the cell against osmotic lysis. The peptidoglycan of *Staphylococcus aureus* is formed up by a backbone alternating N-acetylglucosamine and N-acetylmuramic acid residues forming pentaglycine bridges between L-lysine and D-alanyl residues of muramic acid. The lysostaphin intention is to disrupt the peptidoglycan's pentaglycine cross-bridge that is made up of five glycine (Gly) residues. Lysostaphin hydrolyses specially between the third and the fourth glycine residues which can be seen in the following structure Figure 12) [6].

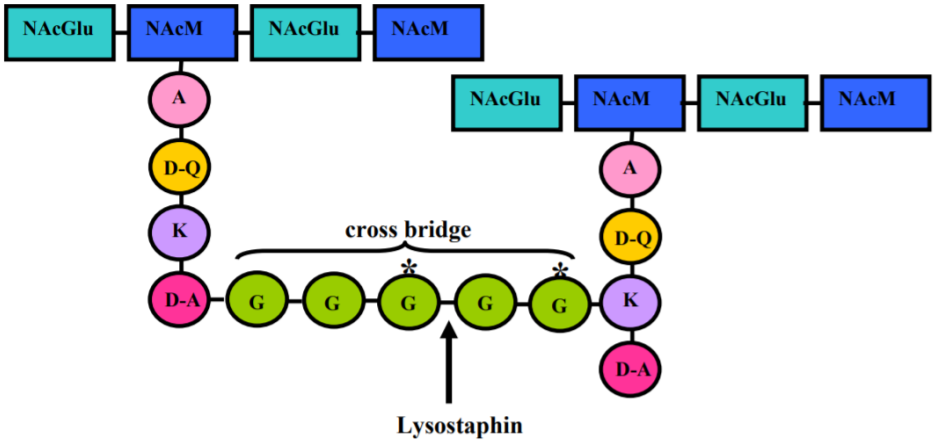

Figure 12: Structure of S. aureus peptidoglycan and common place where hydrolysis of lysostaphin occurs on the staphylococcal peptidoglycan (NacGlu, N-acetyglucosamine; NacM, N-acetylmuramic acid; A, L-alanine; D-Q, D-glutamine; K, L-lysine; D-A, D-alanine; G, L-glycine) [6].

Luckily, lysostaphin studies have shown a positive specific effect against staphylococcal pathogens and this bacteriocin could help to protect us from life-threatening infections whether in its own form or in a mixture with other antibacterial additives [6].

In the study by Wu et al. [58], there was an investigation of effectiveness of lysostaphin and antibiotics like vancomycin and oxacillin on formed *S. aureus* biofilms. It was found out that lysostaphin destroys *S. aureus* biofilms immediately and is more active than the mentioned conventional antibiotics. They examined polystyrene 96-well tissue culture plates covered by biofilms being in contact with dilutions of lysostaphin, oxacillin and vancomycin for twenty-four hours. They measured the biofilm absorbances at 650 nm to find out the kinetic activity of these three substances during 0 to 3 and 24 hours. There were the dilutions of lysostaphin (0.8 to 200 µg/ml), vancomycin (3.2 to 800 µg/ml) and oxacillin (1.6 to 400 µg/ml) in incubator with the tissue culture wells containing the biofilms of *S. aureus*. The results showed that the measured absorbance of biofilms treated by lysostaphin decreased from 0.35 to 0.125 after 3 hours. The absorbance almost dropped the baseline at 0.04 after 24 hours while the biofilms were in a dose of lysostaphin of 6.25 µg/ml in PBS. However, the biofilm absorbances treated by vancomycin and oxacillin hardly showed any change in 24 hours. Although the antibiotic dilutions were as 400 µg of oxacillin/ml and 800 µg of vancomycin/ml in PBS, the absorbance stayed at point about 0.325 (Figure 13).

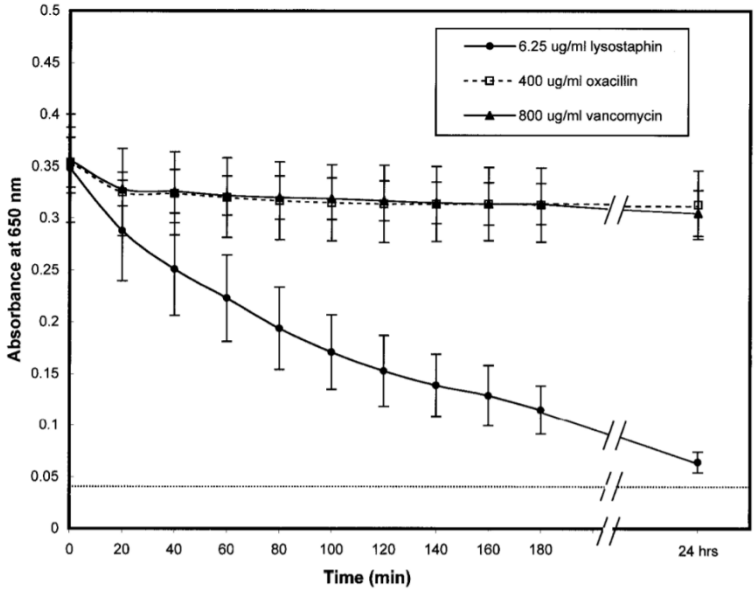

Figure 13: Graph showing the dependence of absorbance on time and the immediate drop in the absorbance of S. aureus biofilms due to lysostaphin action [58].

Another study by Xue and colleagues [2], presents lysostaphin-loaded hydroxyapatite/chitosan composite bone cement. They tested lysostaphin antimicrobial activity against MRSA released from cement samples that were left in normal saline for different times (0, 1, 3, 5, 7, 9 and 11 days). The antibacterial activity assay was performed with 1 ml of MRSA bacteria suspension with agarose culture media. There were 1 non-lysostaphin cement sample and 7 lysostaphin-loaded cement samples put on the Petri dish incubated at 37 °C for 16 hours. The results were indicated due to the inhibitory zones appearing on the Petri dish. The inhibitory zones were visible around cement samples of 0, 1, 3, 5, 7 and 9 day (Figure 14). This testing showed good releasing feature of lysostaphin-loaded cement and its strong activity against MRSA.

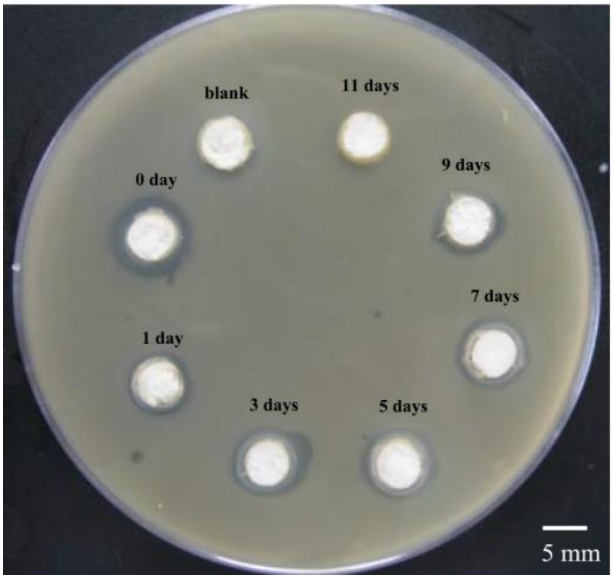

Figure 14: Antibacterial activity of lysostaphin-loaded cement against MRSA proved by inhibition zones in different times [2].

Novel Triblock Copolymer-based CPC

Recently, commonly used water or salt solution as the liquid phase in CPC preparation was replaced by thermosensitive PLGA-PEG-PLGA triblock copolymer in order to improve CPC rheological, morphological and degradation properties [30]. PLGA-PEG-PLGA, triblock copolymer, consists of two monomers. The first monomer is composed of poly(lactic acid) and poly(glycolic acid) and the second is presented by poly(ethylene glycol) [30]. The synthetis of the PLGA-PEG-PLGA copolymer is shown in the reaction (Figure 15).

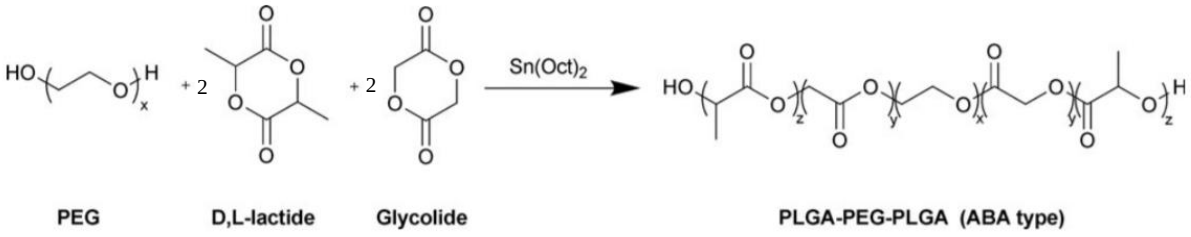

Figure 15: The synthesis of the PLGA-PEG-PLGA triblock copolymer using tin octoate as a catalyst [59].

The PLGA block is hydrophobic and the PEG block is hydrophilic. This thermosensitive copolymer is significant because of its properties, which are non-toxicity biocompatibility, biodegradability. The soluble PLGA-PEG-PLGA stays in a sol form in an environment between 2 to 15°C. However, it changes into a water insoluble gel at body temperature [60]. Amphiphilic copolymer is able to form micelles in water thanks to the hydrophobic behavior of PLGA part [30]. As the temperature of the solution increases, the micelles get stronger and aggregates of micelles appear [60]. PLGA-PEG-PLGA naturally degrades in Krebs's cycle [30]. The copolymer also serves as an excellent drug delivery system for both hydrophilic and hydrophobic drugs [60]. When the copolymer is added to α-TCP cements, it controls their visco-elastic properties and prevents the washout of the cements when submerged in liquids [30][61].

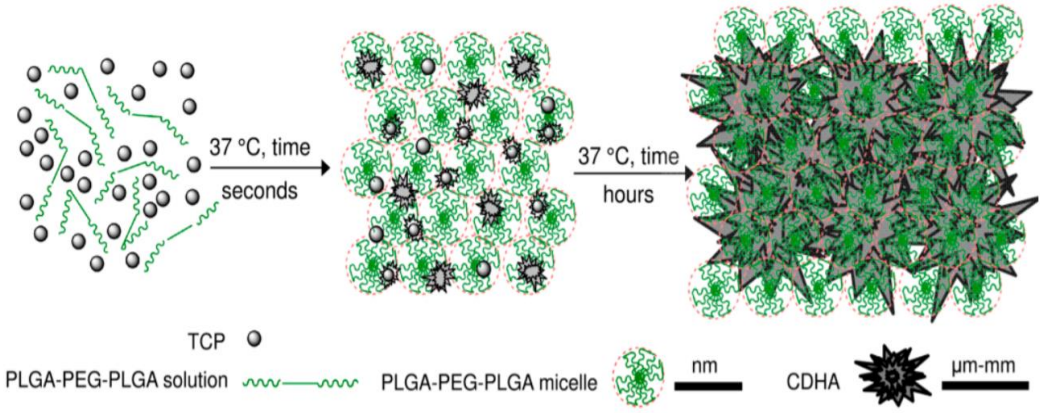

Figure 16: Scheme representing mixing of copolymer with α-TCP followed by fast micellization of copolymer at 37 °C and precipitation of CDHA [30].

As shown in the Figure 16, we can see the fast gelation of copolymers, while the setting of α-TCP lasts for hours to several days [30].

Within proposed work, the copolymer-based CPC will be lysostaphin-modified in order to enhance its antimicrobial efficiency in the osteomyelitis treatment.

3 MAIN GOALS OF THE WORK

The main aim of this work was to optimize antibacterial activity of bone cement that would be injectable and biocompatible. The antibacterial efficacy was ensured by addition of bactericidal enzyme lysostaphin to a mixture of α-tricalcium phosphate and PLGA-PEG-PLGA copolymer water solution, that are the major materials creating phosphate bone cement. Another goal of this work was to evaluate the releasing feature of lysostaphin and model proteins lysozyme and albumin from prepared phosphate bone cement in time in order to understand their release mechanism. In order to evaluate antibacterial properties of lysostaphin-loaded CPC, there was performed antibacterial test by disk-diffusion, dilution and plate method. The last measurement of this work was done to determine functional groups present in the molecules of the prepared protein-loaded CPCs samples by ATR-FTIR spectroscopy.

4 EXPERIMENTAL PART

4.1 Chemicals

- α-TCP, Alpha-Tricalcium Phosphate was prepared by Dr. Edgar B. Montufar at CEITEC BUT (Median size = 12.82 μm)
- PLGA-PEG-PLGA triblock copolymer was prepared by Ing. Klára Lysáková at CEITEC BUT (PDI = 1.09, M_n = 5 665 g.mol^{-1})
- Physiological solution (intravenous 0.9% NaCl solution for infusion) was purchased from Braun (Germany)
- Recombinant lysostaphin LYSSTAPH-S was prepared at Veterinary Research Institute (Brno) by doc. Luboš Janda
- Albumin human (≥ 96%) was purchased from Sigma-Aldrich (MO, USA)
- Lysozyme human (≥ 90%) was purchased from Sigma-Aldrich (MO, USA)
- Staphylococcal strains (MRSA) were prepared by Veterinary Research Institute (Brno)
- Bacterial strains (SA, MRSA, E. coli) were prepared by Mendel University (Brno)
- Mueller-Hinton medium was prepared at Mendel University (Brno)
- Bradford Reagent (for 0.1 - 1.4 mg·ml^{-1} protein) was purchased from Sigma-Aldrich (MO, USA)
- Ultrapure water (Ultrapure watere of Type I according to ISO 3696) was prepared on Miillipore purification system (MilliQ Academic, Millipore, France)

4.2 Equipments

- UV-VIS Spectrophotometer Biochrom Libra S22 (United Kingdom)
- Analytical scales Adventurer Pro AV64 (OHAUS, Switzerland)
- Lyophilizator /Freeze Dryer Epsilon 2-10D LSC plus (Martin Christ, Germany)
- Cell Cultural Incubator CO2cell (BMT Medical, Czech Republic)
- Cooled Incubator VWR INCU-Line (United Kingdom)
- Esco Aistream Class II, Biological Safety Cabinets (Singapore)
- FTIR Spectrometer VERTEX 70v (Bruker, MA, USA)
- Magnetic stirrer MIX 8 XL (2mag magnetic motion, Germany)
- Millipore purification system (MilliQ Academic, Millipore, France)
- Biological Thermostat BT 120
- Desiccator (Sicco, Germany)
- Multiskan Spectrophotometer
- Colony counter
- Automatic pipettes (Hirschmann Laborgeräte, Germany)

4.3 Sample Preparation

4.3.1 General Preparation of Calcium Phosphate Cement

The phosphate bone cement was prepared by mixing a solid phase (α-TCP) and a liquid phase (copolymer PLGA-PEG-PLGA in 0.9 % solution of NaCl) which is shown in the following scheme (Figure 17). The used L/P ratio of these materials was 1:2. L means liquid (copolymer in NaCl solution), P is for α-TCP powder. The amount of copolymer in the NaCl solution was 15 %. First, the α-TCP powder was activated by drying in a drying room at 110 °C for 24 hours. At the same time, the required amount of the copolymer was dissolved and mixed in the solution of NaCl in a cooled incubator at 12°C (600v) for 3 days. This quite low temperature was optimal for the dissolution rate. After 3 days these 2 materials were mixed until the cement was homogeneous.

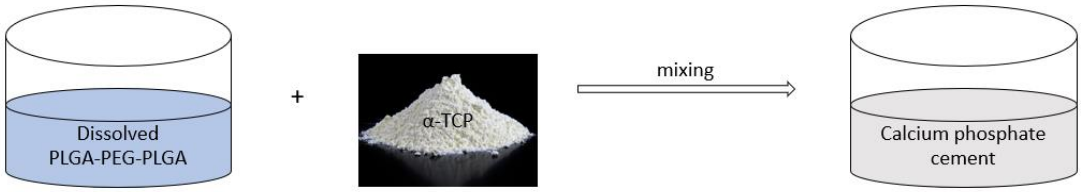

Figure 17: Scheme presenting preparation of calcium phosphate cement.

4.3.2 Optimization in Preparation of Protein-loaded CPC

4.3.2.1 *Samples A Preparation for Release of LYSSTAPH-S*

CPC samples loaded by lysostaphin LYSSTAPH-S were prepared for measurerement of this enzyme amount released from the cured cement in time. The size of these samples was 2×6 mm and the number of samples was 7. LYSSTAPH-S was purchased in lyophilized form in an eppendorf tube followed by its dilution in NaCl solution. The cement was prepared according to the previous general preparation of CPC (4.3.1). The calculated LYSSTAPH-S solution was dissolved in prepared PLGA-PEG-PLGA solution followed by α-TCP powder addition. These materials were mixed well and injected into 2×6 mm molds via syringe. The addition of lysostaphin solution greatly diluted the cement resulting in a slow curing of the cement in the incubator. Even so, the samples were very fragile and disintegrated as shown in the next picture (Figure 18).

Figure 18: The fragile and disintegrated LYSSTAPH-S lysostaphin-loaded CPC samples after curing in the incubator.

4.3.2.2 *Samples B Preparation for Release of Lysozyme and Albumin*

Lysozyme and albumin were used to serve as model proteins for release experiment. Lysozyme molecular weight (14 $kg.mol^{-1}$) is lower than LYSSTAPH-S molecular weight (25 $kg.mol^{-1}$), and on the contrary, albumin molecular weight (67 $kg.mol^{-1}$) is higher. The fact that the molecular weight of lysostaphin LYSSTAPH-S is among the molecular weights of the mentioned model proteins was used. It was also realised to prepare bigger samples. There was weighted 2600 μg of lysozyme and albumin and both of them were diluted in 0.5 ml of NaCl solution. Required number of samples was 8. There were prepared required amounts of polymer solution and α-TCP powder. 0.5 ml of solution with lysozyme was pipetted into the polymer solution and then α-TCP powder was added. The material was mixed for 40 s. The formed paste was pushed into 3 ml syringe and there were injected samples into prepared 2×10 mm molds on Petri dish. Albumin samples were prepared the same way. The samples were put into incubator (37 °C) for one hour. The additon of 0.5 ml of solution diluted the paste very much and more samples were produced than desired amount (14 samples) resulting in a decrease of the concentration in the individual sample. Another problem appeared with a decrease of the concentration of the polymer solution (10 %) by adding the solution of protein which was reflected in the slower setting feature of the samples in the incubator.

4.3.2.3 *Samples C Preparation for Release of Lysozyme and Albumin*

To prevent previous negative results and problems there was used only a half amount of materials and there was prepared 20 % solution of polymer so the addition of protein solution dilutes it at required 15 % of polymer solution. There was weighted 2600 μg of lysozyme and albumin as in previous preparation. The proteins were diluted in only 0.2 ml of NaCl solution. Then all materials were mixed as mentioned previously and there were formed fewer samples (2×10 mm) which we wanted to achieve. The samples were put into the incubator for one hour to be cured.

4.3.2.4 *Samples D Preparation for Release of LYSSTAPH-S*

The samples D were prepared the same way as the samples C with 20 % solution of polymer. There were available Eppendorf tubes with 1500 μg of lyophilized LYSSTAPH-S. There were taken two Eppendorf tubes with LYSSTAPH-S and each amount was stirred in 0.12 ml of NaCl solution. Both volumes were put together so the final amount in the Eppendorf tube was 3000 μg of LYSSTAPH-S in 0.24 ml of NaCl solution. This volume was pipetted into polymer solution, powdered α-TCP was added and everything was mixed together. The formed paste was put into syringe and it was injected on the Petri dish into prepared 2×10 mm molds. The samples were put into incubator for one hour to be cured.

4.4 Methods

4.4.1 Antibacterial Activity Assay

First measurement at VRI

First, the antibacterial activity of lysostaphin LYSSTAPH-S released from the CPC was tested against MRSA. The assay was performed by agar disk-diffusion method at Veterinary Research Institute in Brno (VRI). The experiment was carried out to provide information about antibacterial activity of lysostaphin. All staphylococcal strains tested were methicillin-resistant *S. aureus* and here are its three sequence types:

- **ST 22 (5921)**
- **ST 8 (244)**
- **ST 395 (PS187)**

Second measurement at MendelU

The second antibacterial activity assay was performed with lysostaphin LYSSTAPH-S and lysozyme-loaded CPC samples against different types of bacteria. The samples with lysozyme serve as a model protein. The assay was performed by disk-diffusion, dilution and plate method at Mendel University in Brno. There were used three types of bacteria:

- ***S. aureus* SA (CCM 4223)**
- **Methicillin-resistant *S. aureus* MRSA (CCM 7110)**
- ***Escherichia coli* EC (CCM 3954)**

4.4.1.1 *Preparation of the Protein-loaded CPCs*

In the first antibacterial assay at VRI, there were prepared 7 different concentrations of LYSSTAPH-S (Table 3). The lyophilized lysostaphin LYSSTAPH-S was mixed in the NaCl solution and further diluted to the required concentrations. One of the concentrations was as a control (K), without the addition of lysostaphin. There were weighed all materials for the CPC according to the general preparation of CPC (4.3.1). There was prepared 1 ml of the CPC of each concentration divided for 3 bacteria.

Table 3: Concentrations of lysostaphin LYSSTAPH-S in each prepared CPC sample.

Number of concentrations	Concentration [µg/sample]
1	130
2	90
3	80
4	50
5	30
6	10
K	0

In the second antibacterial assay at Mendel University, there were prepared 4 concentrations of lysostaphin and 2 concentrations of lysozyme (Table 4, Table 5). There was prepared one concentration as a control (Ø), without the addition of lysostaphin or lysozyme. The original amount of lyophilized lysostaphin LYSSTAPH-S was mixed in the NaCl solution and further diluted to the required concentrations. The lysozyme concentrations were prepared by dissolving the required amounts of lysozyme in the NaCl solution. The CPCs were prepared according to the preparation of the samples D (4.3.2.4) with 20% polymer solution. There was formed 1 ml of the CPC of each concentration divided for 3 bacteria for the disk- diffusion method and for 1 bacterium for the dilution method.

Table 4: Concentrations of lysostaphin LYSSTAPH-S in each prepared CPC sample.

Number of concentrations	Concentration [µg/sample]
LP1	300
LP2	150
LP3	75
LP4	30
Ø	0

Table 5: Concentrations of lysozyme in each prepared CPC sample.

Number of concentrations	Concentration [µg/sample]
LS1	300
LS2	150

4.4.1.2 *Disk-Diffusion Antibacterial Assays*

The disk-diffusion metod was used to detect the susceptibility of the bacterial strains to lysostaphin and lysozyme loaded in CPC. The measurement was performed on Petri dishes with prepared MH medium and bacterial cultures. The susceptibility of the bacterial strains to the tested proteins loaded in CPCs was evaluated by the formation of inhibition zones around the samples after incubating the Petri dishes for 24 and 48 hours. The inhibition zones were formed by diffusion of the proteins placed on the surface of the medium and bacterial cultures.

In the first antibacterial assay at VRI, there were tested three types of MRSA. The testing was performed on the Petri dishes with blood agar. The MRSA bacteria suspension diluted at 1-2 × 10^8 CFU/ml by the NaCl solution were spread on the agarose medium on the Petri dishes. Meanwhile, the CPCs were formed by mixing the weighed and prepared materials (α- TCP, PLGA-PEG-PLGA) with pipetted amounts of lysostaphin. The mixed content was pushed into syringe using a spatula. Then 0.25 ml of the cement was injected on each prepared Petri dishes with different type of bacteria (Figure 19). This was repeated with each LYSSTAPH-S concentration. All Petri dishes with injected cement were put into biological thermostat heated at 37 °C for 24 and 48 hours to see if inhibition zones were formed.

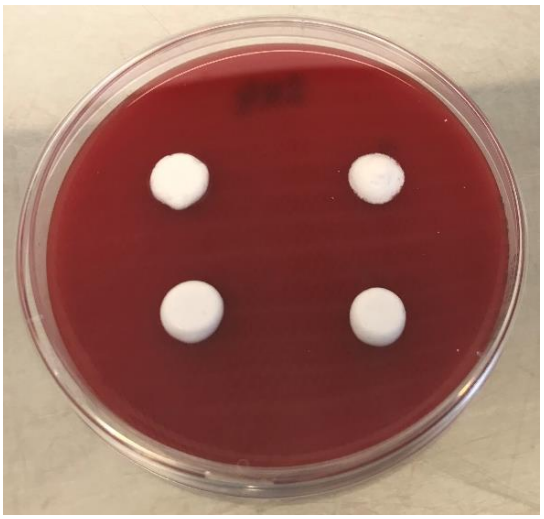

Figure 19: The LYSSTAPH-S lysostaphin-loaded phosphate cement injected on the Petri dish with blood agar and suspension of MRSA.

The second disk-diffusion antibacterial assay at Mendel University was carried out in a very similar way. There was used Mueller-Hinton (MH) agar instead of the blood agar. The bacterial cultures were spread all over the Petri dishes and LYSSTAPH-S and lysozyme-loaded CPCs were formed. Then 0.25 ml of each CPC was injected on the Petri dish with different type of bacteria and into Eppendorf tube for the dilution method (only with MRSA). This was repeated with each protein concentration and with the control sample too. There were applied control antibiotics on the Petri dishes as an additional control. Penicillin was used for *S. aureus*, vancomycin for MRSA and amoxycilin for *E. coli*. All Petri dishes with injected cement were put into biological thermostat (37 °C) for 24 hours to see if inhibition zones were formed.

4.4.1.3 *Dilution Antibacterial Assay*

The dilution method was used to determine the number of bacteria in Eppendorf tubes with protein-loaded CPC immersed in MH medium with bacteira. The experiment was carried out by measuring the absorbance of the solutions after their incubation (37 °C) for both 24 and 48 hours by Multiskan spectrophotometer.

The Eppendorf tubes with injected CPCs were filled with 2 ml of MH medium with MRSA bacterium of a cell density of 1-2 × 10^6 CFU/ml. One Eppendorf tube was prepared only with a solution of MH medium and bacteria for comparison.

4.4.1.4 *Plate Antibacterial Assay*

The plate method consisted in determining the number of grown colonies on the Petri dishes. There was used a diluted amout of the solution from the previous Eppendorf tubes and it was spread on the Petri dishes with MH agar. The formed bacterial colonies were counted by a colony counter after incubation of the Petri dishes for both 24 and 48 hours at 37 °C.

There were used the samples prepared for the dilution assay in this experiment. 100 ml of the solution was taken from each Eppendorf tube, and after decimal dilution, the solution was applied on Petri dishes with MH agar.

4.4.2 Protein Release Experiments by UV-VIS Spectrophotometry

The UV-VIS spectrophotometer (Figure 20) was used to measure the released amount of proteins from the cured calcium phosphate cements in time. The measurement was performed at 595 nm with Bradford reagent. The Bradford reagent was used to interact with proteins and move their absorption maxima from 280 nm to 595 nm. There were used cuvettes with dosed ratios of Bradford reagent and sample according to the released amount of protein. The solution turned blue as the Bradford reagent bound to the proteins (Figure 21). The following table (Table 6) shows the pippeted volumes and the ratios of Bradford reagent and sample.

There were used previously mentioned samples B, C and D (4.3.2.2, 4.3.2.3, 4.3.2.4) loaded by lysozyme, albumin and lysostaphin LYSSTAPH-S. All of the cured samples were weighed on analytical scales to found out how much protein they should contain due to the original used quantities. These samples were immersed separately in vials with 3 ml of NaCl solution and these were put into incubator (37 °C). The NaCl solution was replaced with fresh NaCl solution after 1, 2, 3, 7, 9, 14, 16, 21 and 35 days to determine the cumulative release of the proteins. Some of the samples were immersed into NaCl solution which, however, was not replaced, and the released amount was measured individually after 0, 1, 7 and 14 days.

Figure 20: UV-VIS spectrophotometer Biochrom Libra S22 used for the release measurement.

Table 6: The pippeted amount and ratio of Bradford reagent and sample.

	Bradford Reagent [µl]	Sample [µl]	Bradford Reagent	Ratio	Sample
Low concentrations (1-10 µg/ml)	500	500	1	:	1
Middle concentrations (10-100 µg/ml)	800	200	4	:	1
High concentrations (50-500 µg/ml)	1000	30	33,3	:	1

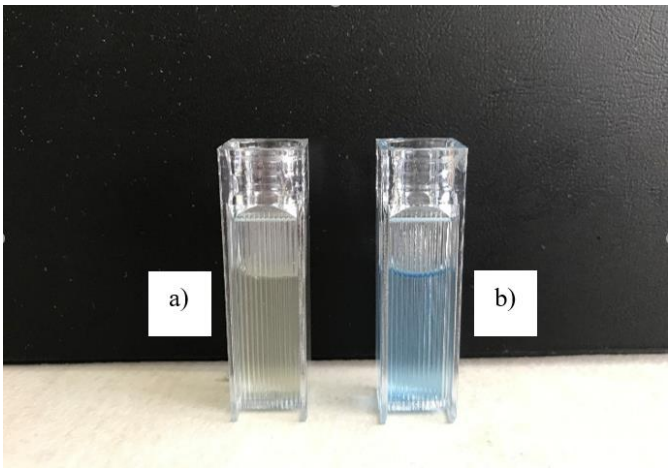

Figure 21: Comparison in the color of the solution in the cuvettes. The first cuvette (a) contains Bradford reagent with NaCl solution (blank), while the second (b) is loaded by Bradford reagent with solution containing released proteins.

4.4.3 ATR-FTIR Spectroscopy Measurement

ATR-FTIR spectroscopy is an abbreviation for Attenuated total reflectance-Fourier transform infrared spectroscopy. The FTIR spectrometer (Figure 22) was used to detect and provide information about the functional groups present in the molecules of the prepared protein-loaded CPCs. The technique is based on the reflection of infrared radiation between the sample and the crystal. There were shot 64 scans for every sample to create their spectra. The spectra were collected over the range 4000 to 600 cm^{-1} under vaccum.

The samples C with lysozyme and albumin and the samples D with LYSSTAPH-S lysostaphin immersed individually in NaCl solution for 0 and 1 day from the previous release experiment were used. The protein-loaded cement samples C and D were freeze-dried and crushed in a mortar. A small amount of the formed powder was poured into the FTIR spectrometer and covered with the ATR crystal.

Figure 22: FTIR spectrometer Bruker VERTEX 70v with ATR crystal used for the measurement.

5 RESULTS AND DISCUSSION

5.1 Calibration of Lysostaphin Solutions by UV-VIS Spectrophotometer

Calibration curves were performed to measure release of the lysostaphin enzyme for different concentrations. The measurement was realised by using a UV-VIS spectrophotometer set at 595 nm in the presence of a Bradford reagent. The Bradford reagent binds to proteins specifically and it moves their absorption maxima from 280 nm (UV zone) to 595 nm (visible light zone). Calibration curves were prepared for low concentration (1-10 µg/ml), middle concentrations (10-100 µg/ml) and high concentrations (50-500 µg/ml). The following graphs (Figure 23, Figure 24, Figure 25) show dependance of absorbances to concentrations.

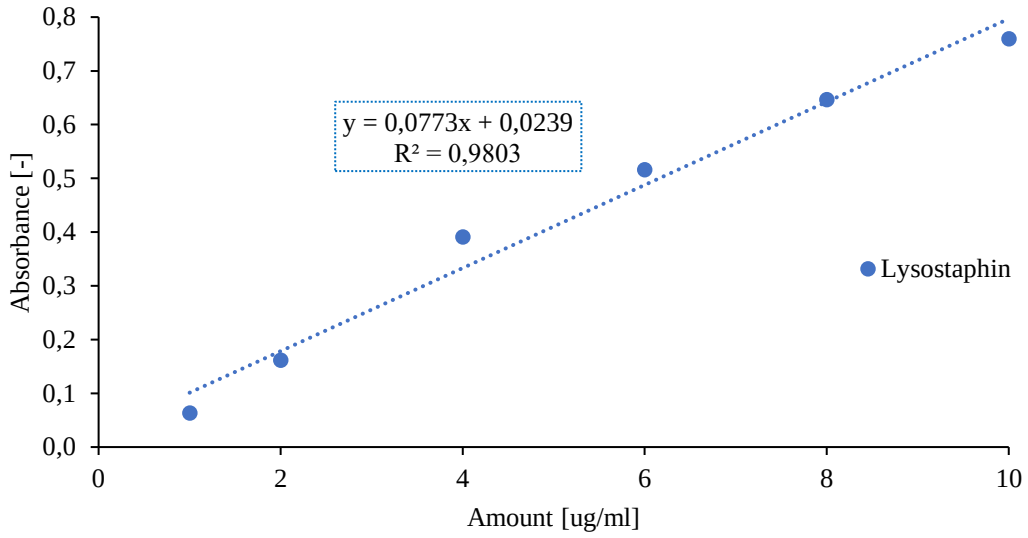

Figure 23: Graph of lysostaphin LYSSTAPH-S calibration curve for low concentrations (1-10 µg/ml).

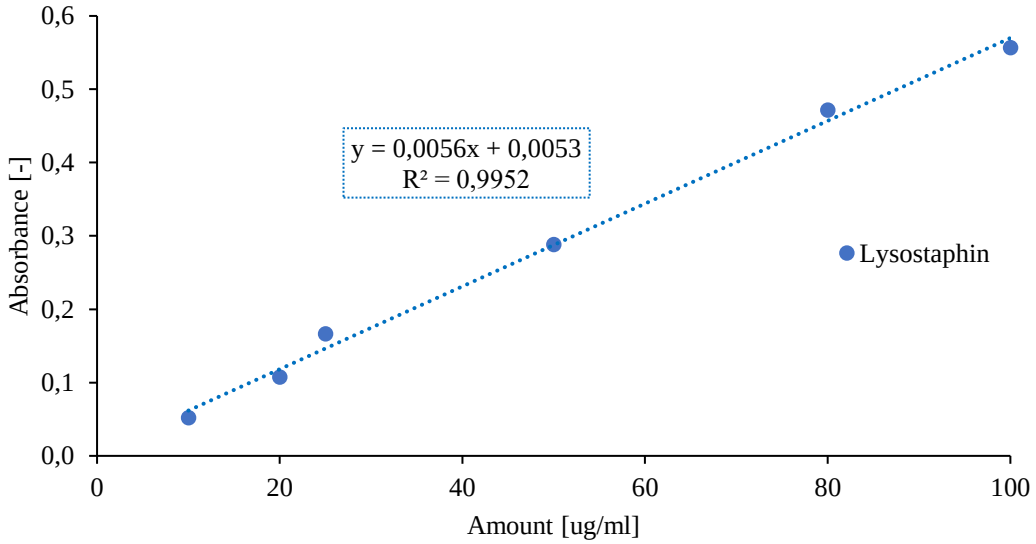

Figure 24: Graph of lysostaphin LYSSTAPH-S calibration curve for middle concentrations (10- 100 µg/ml).

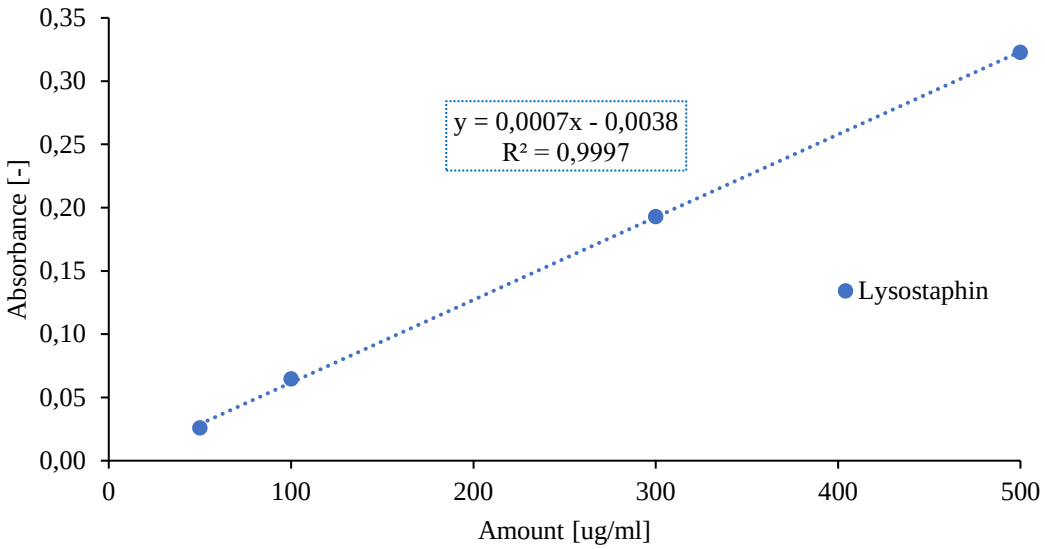

Figure 25: Graph of lysostaphin LYSSTAPH-S calibration curve for high concentrations (50- 500 µg/ml).

5.2 Calibration of Lysozyme and Albumin by UV-VIS Spectrophotometer

Calibration curves were measured with lysozym and albumin for the same purpose as previous lysostaphin curves. Calibration curves were prepared for low concentratios (1-10 µg/ml), middle concentrations (10-100 µg/ml) and high concentrations (100-1000 µg/ml). These calibration curves (Figure 26, Figure 27, Figure 28) were measured by Ing. Klára Lysáková (CEITEC BUT) [62].

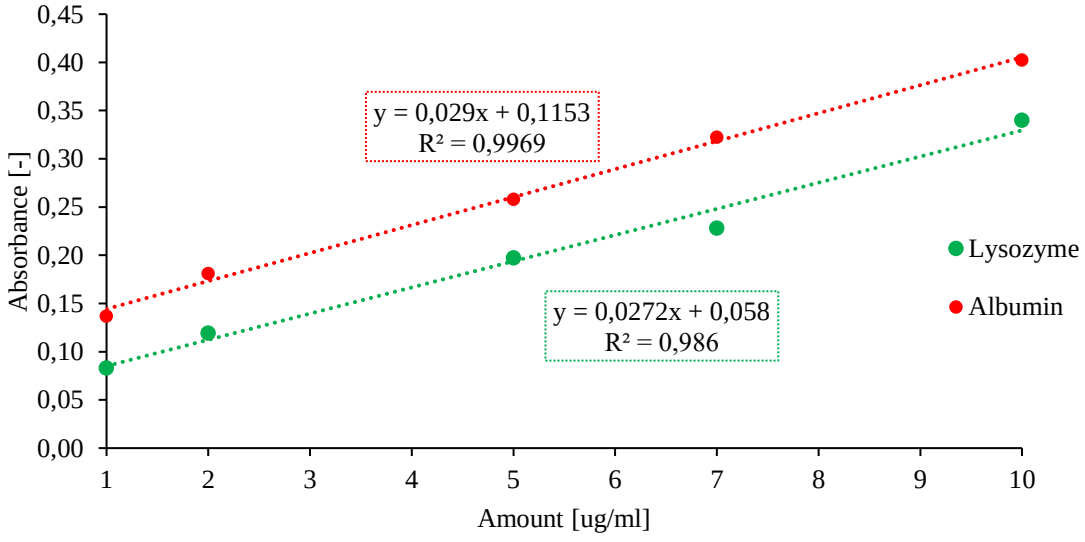

Figure 26: Graph of lysozyme and albumin calibration curves for low concentrations (1-10 µg/ml) [62].

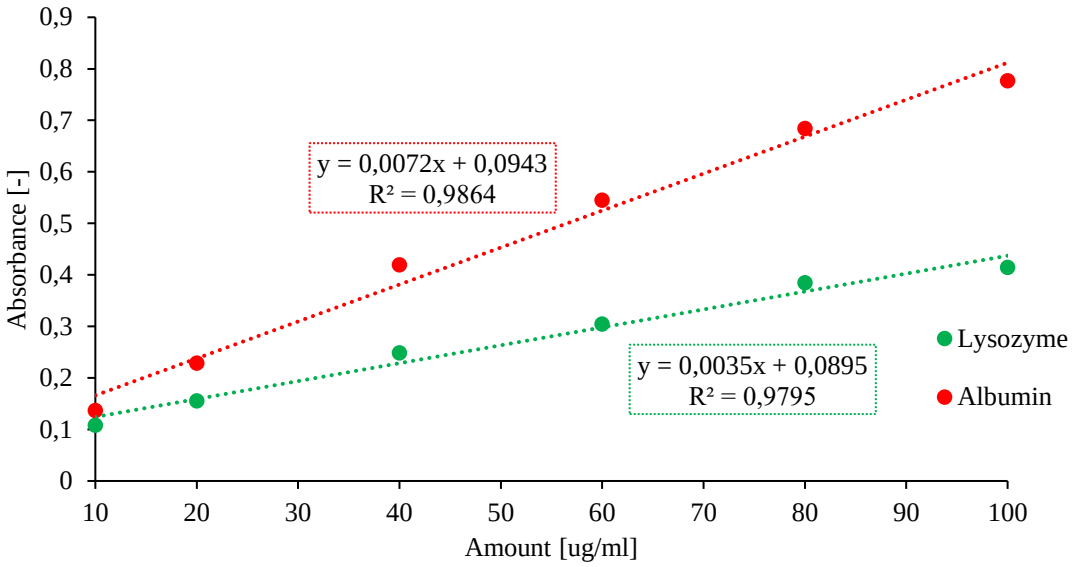

Figure 27: Graph of lysozyme and albumin calibration curves for middle concentrations (10-100 µg/ml) [62].

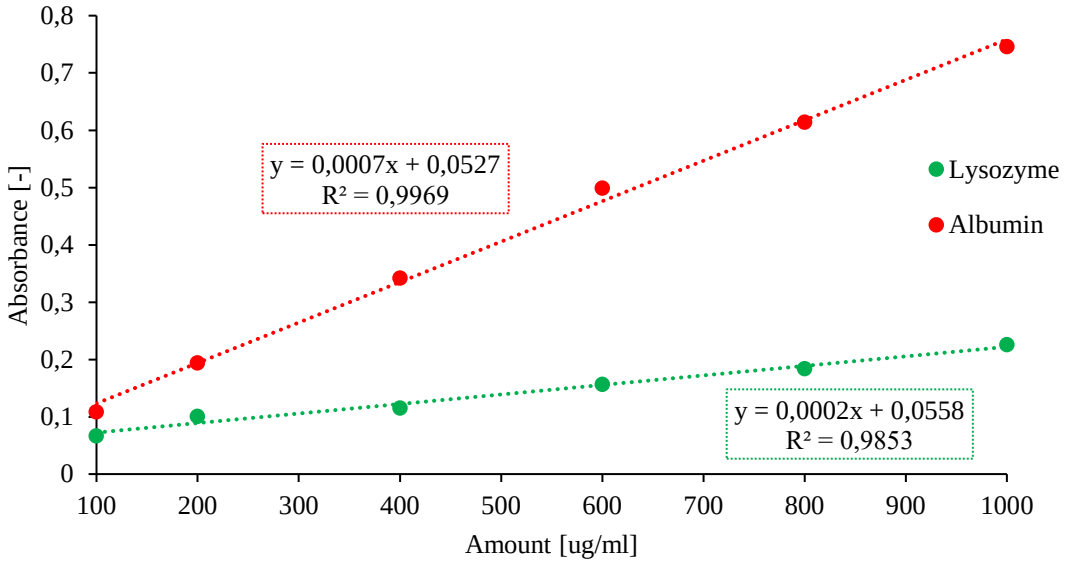

Figure 28: Graph of lysozyme and albumin calibration curves for high concentrations (100-1000 µg/ml) [62].

5.3 Protein Release Experiments

The released amounts of proteins from CPC into NaCl solution were calculated according to the equations of the calibration curves depicted above. The relative amount of protein was calculated by dividing the released amount of protein by the total amount loaded in the CPC. The cumulative curve was based on the 35 days data (1, 2, 3, 7, 9, 14, 16, 21, 35 days). The released amount was calculated for each time point by adding all the values before that time. The individual curve was generated by the 14 days data (0, 1, 7, 14 days) and the data were plotted for each time point as they were. Lysozyme and albumin were used as model proteins for lysostaphin LYSSTAPH-S release kinetics.

5.3.1 The B Samples Release Behavior

The cumulative release curve with the samples B loaded by lysozyme and albumin showed that about 27.35% of lysozyme was released in 21 days. The samples were then left unmeasured for a longer period of time and were measured after another 14 day, but there was nothing more released. The individual curve showed that the released amount was also 27.35% when released after 24 hours, 24.61% when released after 7 days, and 28.52% when released after 14 days. The albumin samples did not release any amounts of this protein even in the cumulative release measurement for 21 days or in the individual release measurement for 1, 7 and 14 days. Each sample was loaded by about 120 µg of either lysozyme or albumin.

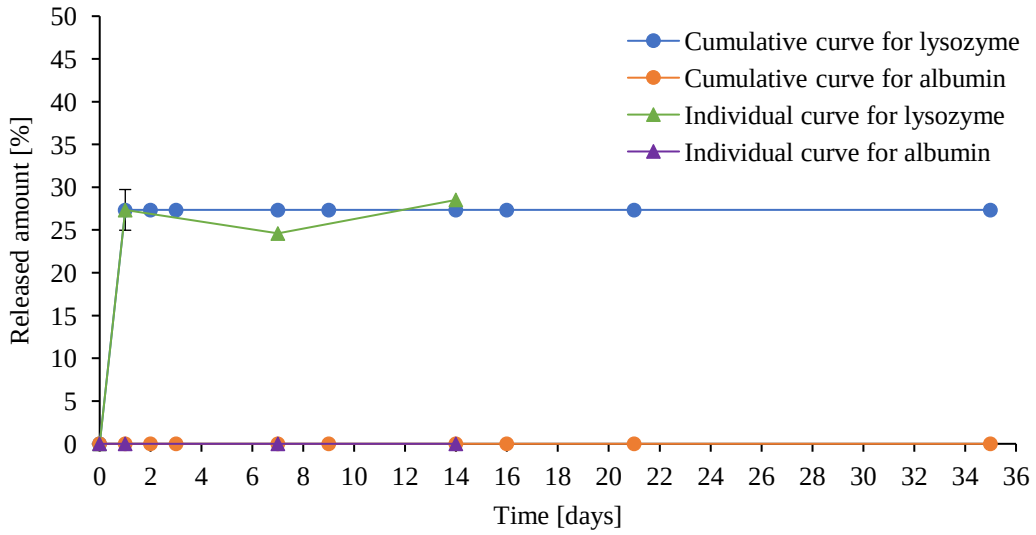

Figure 29: The released amounts of lysozyme and albumin (original amount in the sample=120 µg) from CPC in time.

5.3.2 The C Samples Release Behavior

The cumulative release curve with the samples C loaded by lysozyme and albumin showed that there was released only 15% of lysozyme in 21 days. The samples were then left without measurement for a longer period of time and were measured after another 14 days, but there was nothing more released. The individual curve showed that the release amount was 14.91% when released after 24 hours, 20.81% when released after 7 days, and 18.7% when released after 14 days. The albumin samples again showed no released amounts of protein in either the cumulative or the individual measurement. Each sample was loaded by about 250 µg of either lysozyme or albumin.

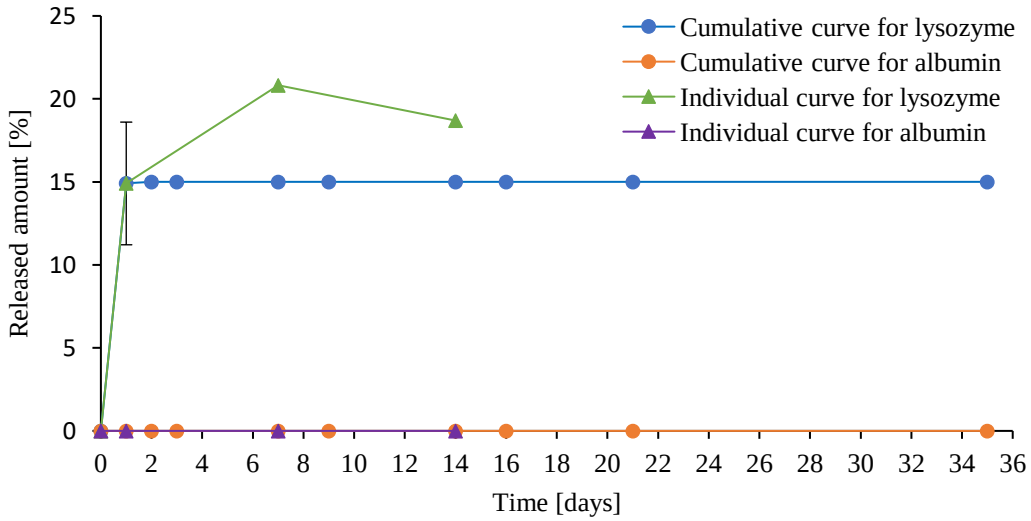

Figure 30: The released amount of lysozyme and albumin (original amount in the sample=250 µg) from CPC in time.

5.3.3 The D Samples Release Behavior

The cumulative release curve with the samples D loaded by lysostaphin LYSSTAPH-S showed that only about 1.26% of LYSSTAPH-S was released in 21 days. The samples were then left without measurement for a longer period of time and were measured after another 14 days. There was detected 2% of lysostaphin released in those 14 days. The total amount released was 3.26%. The individual curve showed that the released amount was 0.76% when released after 24 hours, 1.76% when released after 7 days, and 2.89% when released after 14 days. Each sample was loaded by about 250 µg of lysostaphin LYSSTAPH-S.

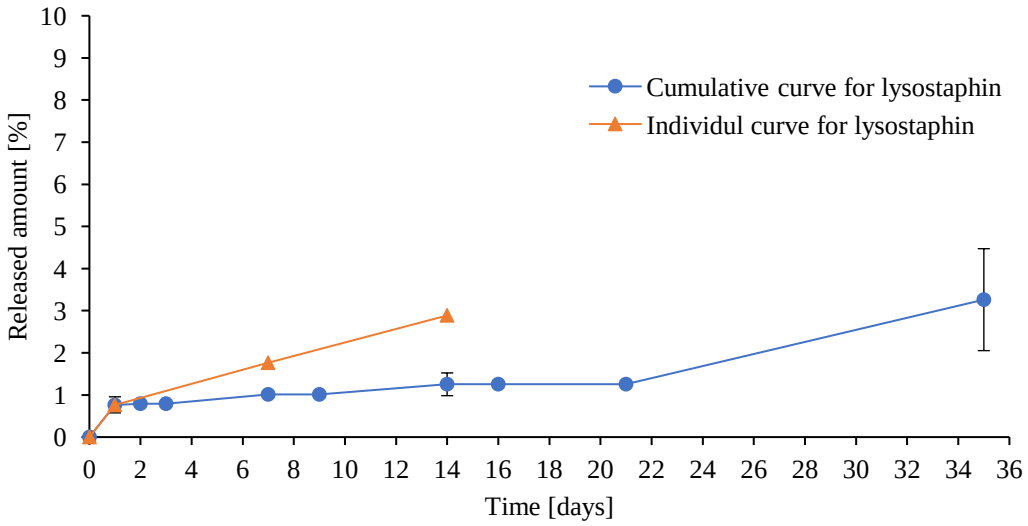

Figure 31: The released amounts of LYSSTAPH-S (original amount in the sample=250 μg) from CPC in time.

There is evidence of poor release kinetics of proteins loaded in the CPCs. The problem may be the high binding affinity of the proteins to CPC and the entrapment of the proteins in CPC pores. The PLGA-PEG-PLGA micelles formed in the CPC can also limit and slow down the proteins release [2]. The molecular weights of lysostaphin, lysozyme and albumin are in the order of tens of $kg.mol^{-1}$, which corresponds to relatively large molecules. These large weights of the proteins can be also a reason for poor release kinetics from CPCs. In the future, an accelerated degradation test of cement in an acidic pH environment simulating osteoclastic bone lysis could be performed to determine if more protein is released, since the acidic environment is needed for CDHA resorbtion. The consideration is whether more proteins would be released after the cement disintegrated. The highest amount of lysozyme and albumin released from samples B and C was after the first day, then the release was constant. When comparing samples B and C, approximately twice as much lysozyme was released from the samples B, which may be related to the lower polymer concentration of the samples B. The amount of lysostaphin LYSSTAPH-S released varied over time, but a very small amount was still released.

5.4 Antibacterial Activity Assay

First measurement provided at VRI

The disk-diffusion antibacterial activity of lysostaphin LYSSTPAH-S against MRSA in the first antibacterial assay (VRI) was observed by the formation of inhibitory zones appearing on the Petri dishes around the injected cements. The staphylococcal strain ST 8 (244) proved to be the most sensitive to LYSSTAPH-S by formation of the widest inhibitory zones. The inhibitory ring of the highest LYSSTAPH-S concentration was about 2 mm thick, the same as the second highest LYSSTAPH-S concentration which means that LYSSTAPH-S was active and inhibited the growth of bacteria. The others had rings of almost identical size (about 1 mm in thickness). The zones increased slightly after incubation for another 24 hours. The concentration 5 and 6 did not form any inhibitory zone because the concentration of lysostaphin LYSSTAPH-S in the CPC sample was pretty low. The following pictures (Figure 32, Figure 33) show the inhibitory zones around the injected LYSSTAPH-S lysostaphin-loaded CPC.

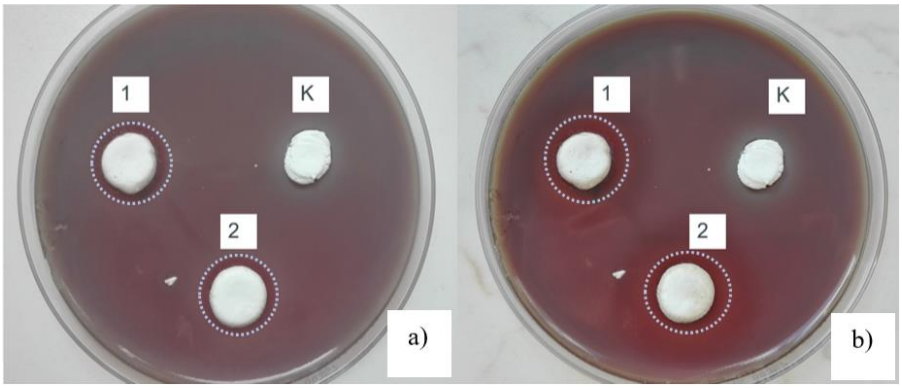

Figure 32: The inhibitory zones formed around CPC of different LYSSTAPH-S concentrations (1-2) having antibacterial activity against MRSA ST 8 (244) after (a) 24 hours and (b) 48 hours.

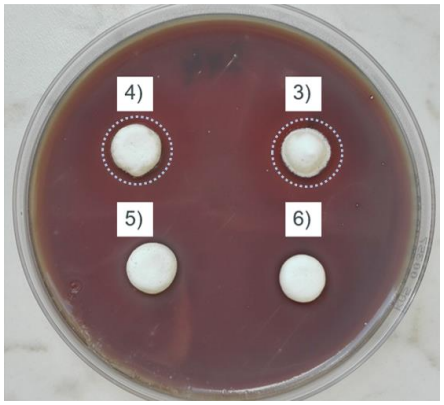

Figure 33: The inhibitory zones formed around CPC of different LYSSTAPH-S concentrations (3-6) having antibacterial activity against MRSA ST 8 (244) after 48 hours.

Second measurement provided at MendelU

The disk-diffusion antibacterial activity of lysostaphin LYSSTAPH-S and lysozyme against SA, MRSA and EC in the second antibacterial assay at Mendel University was observed by the formation of inhibitory zones appearing on the Petri dishes around the injected cement samples. As shown in the photo (Figure 34), there was probably a problem, because the inhibitory zones were formed around the control CPCs with no addition of antibacterial lysostaphin or lysozyme. It is not clear whether an error occurred during the preparation of the CPCs, which is quite out of the question. What else could have caused this problem is for example, a poorly prepared MH medium or the high acidity of PLGA-PEG-PLGA polymer which is one of the materials forming CPCs. Another interesting fact is that all the formed inhibitory zones were almost equally wide although there were different concentrations of LYSSTAPH-S or lysozyme loaded in the CPCs. As far as EC bacteria are concerned, no zones of inhibition have been created, which means that neither lysostaphin LYSSTAPH-S nor lysozyme are effective against this Gram-negative bacterium. The small disks in the middle of the Petri dishes are the control ones with antibiotics.

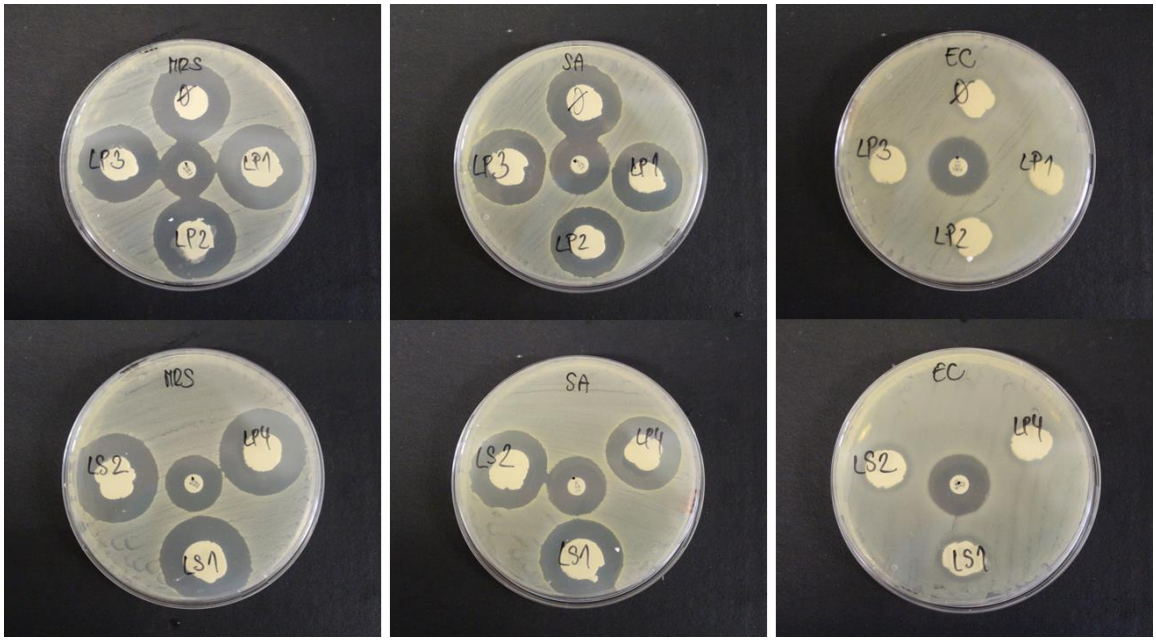

Figure 34: The inhibitory zones formed on the Petri dishes with MRSA, SA and EC bacteria around the injected CPCs with lysostaphin LYSSTAPH-S and lysozyme.

The dilution method was carried out to determine and compare the amount of MRSA bacteria in the Eppendorf tubes with injected CPCs or only with a solution of bacteria (control). The amounts were detected by measuring absorbances of the solutions in the Eppendorf tubes. The measurement turned out quite in the same way as in the disk-diffusion method, when the control cement also had an antibacterial effect and the protein-loaded CPCs worked almost the same despite different concentrations. The following graph (Figure 35) shows the decrease in absorbance after 24 hours which means that LYSSTAPH-S and lysozyme quite reduced the amount of MRSA. The absorbance increased greatly with the bacteria-only solution after next 24 hours while the absorbance in the solution with CPCs increased slightly.

As can be seen in Figure 35, the control cement (0) without antimicrobial addition worked in the same way as those with proteins.

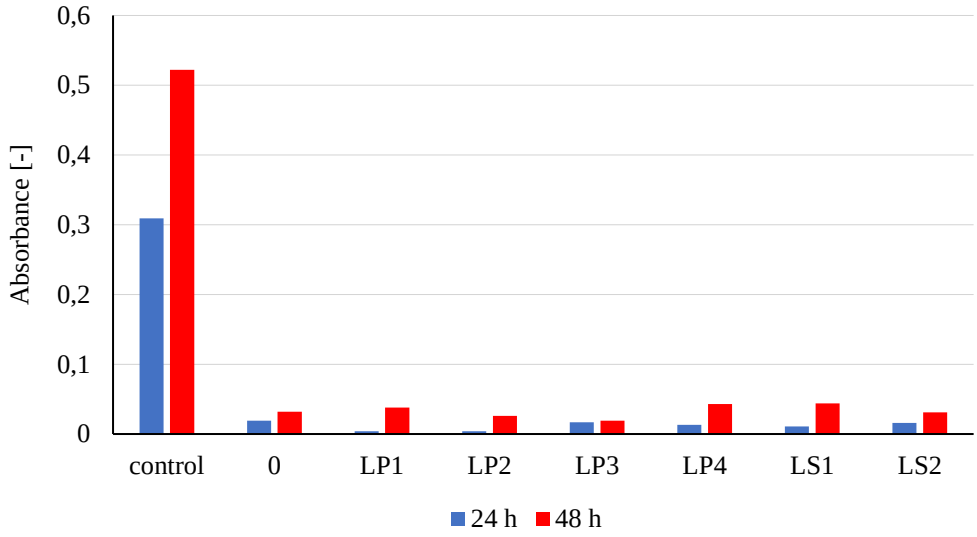

Figure 35: Graph showing the increase and decrease of absorbance determining the amount of MRSA bacteria.

The plate method was performed to compare the number of grown bacterial colonies on the Petri dishes. For this experiment, there were used the solutions with protein-loaded CPCs and the control solution in Eppendorf tubes from the dilution experiment. A certain amount of the solutions was applied on the Petri dishes and incubated for 24 hours. Then, the grown colonies of bacteria were counted by the colony counter. The results were expressed as CFU/ml (colony- forming unit/ml) in the graph (Figure 36). As shown in the graph, there appeared bacterial colonies (9.64×10^7 CFU/ml) only on the Petri dish with the control bacterial solution without addition of CPC. The grown colonies of the control bacterial solution can be seen in the photo (Figure 37).

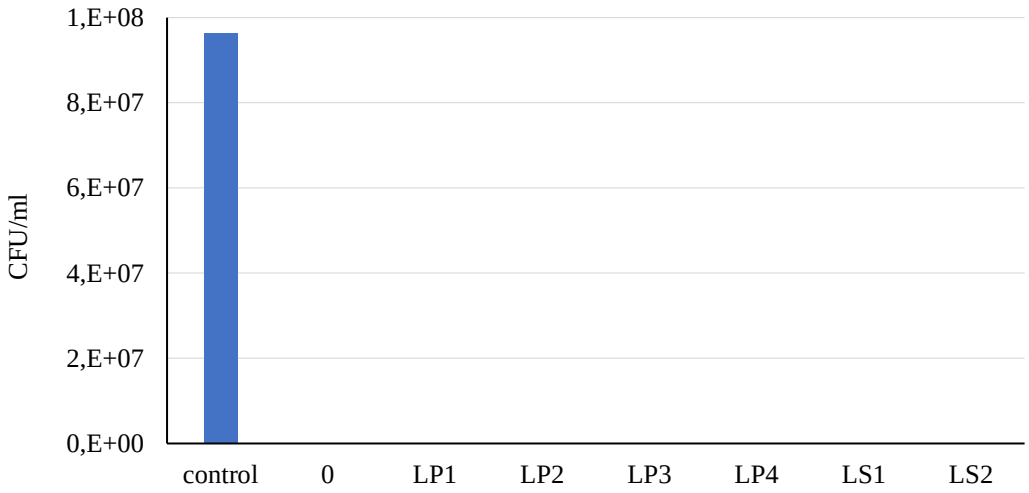

Figure 36: Graph showing the growth of MRSA colonies only on the Petri dish with the control bacterial solution.

The control cement (0) without lysostaphin or lysozyme addition killed all the bacteria which as was mentioned before is an inexplicable error. The protein-loaded CPCs showed the same result.

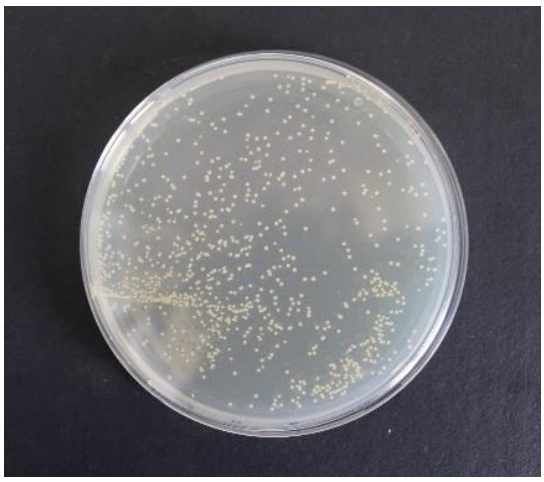

Figure 37: The grown MRSA colonies of control bacterial solution after incubation for 24 hours.

5.5 ATR-FTIR Measurement

The ATR-FTIR measurement was performed to identify the functional groups present in the molecules of the prepared protein-loaded CPC. The measurement was carried out by FTIR spectrometer with ATR crystal under vacuum. The spectra were collected over 4000 cm^{-1} to about 600 cm^{-1} (Figure 38, Figure 39).

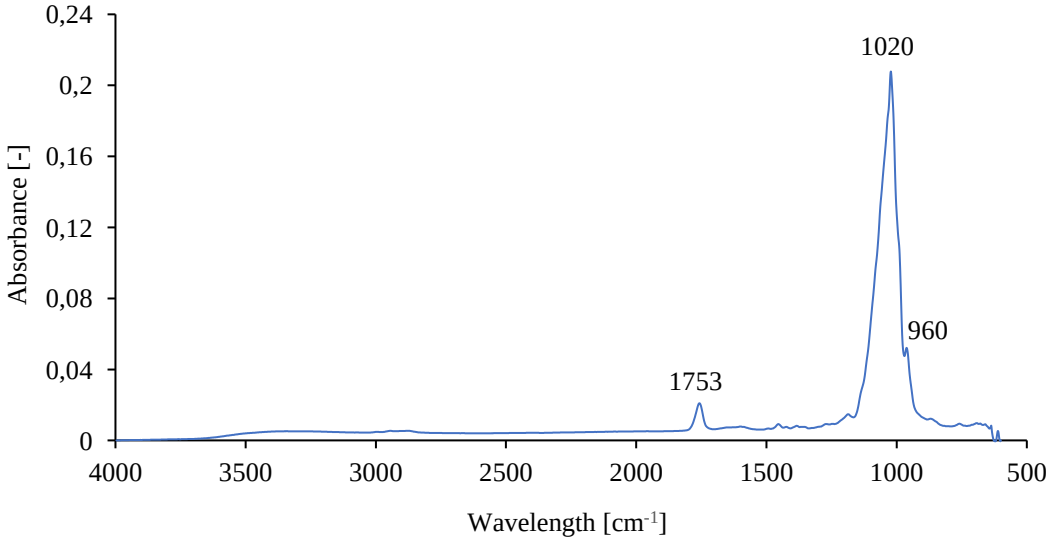

Figure 38: Graph of ATR-FTIR spectrum of LYSSTAPH-S lysostaphin-loaded CPC.

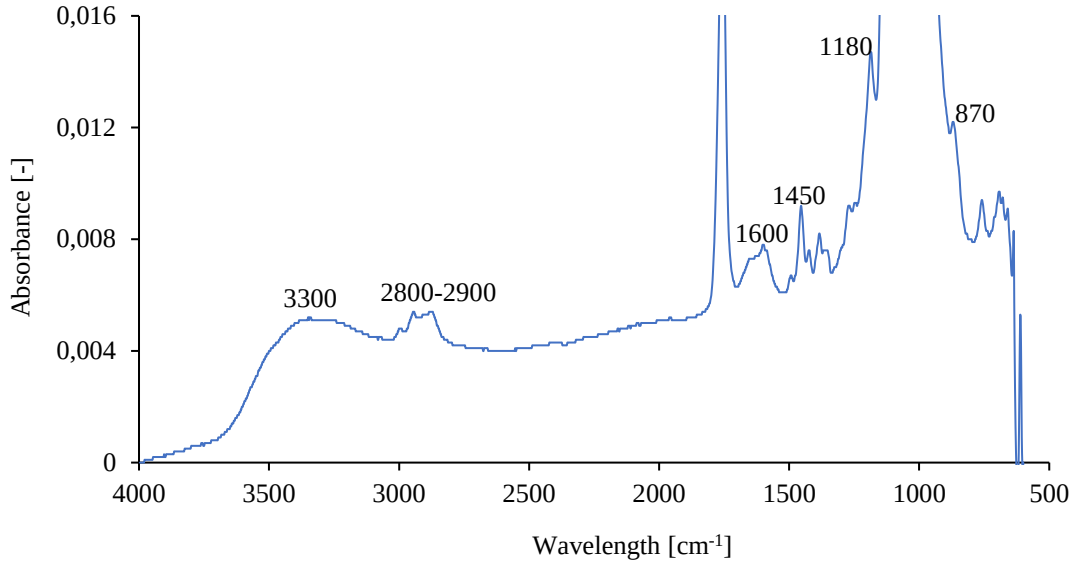

Figure 39: Graph of ATR-FTIR spectrum of LYSSTAPH-S lysostaphin-loaded CPC with lower intensity.

Figure 38 and Figure 39 show the FTIR spectrum of LYSSTAPH-S-loaded CPC sample. The characteristic peak at 1753 cm^{-1} was attributed to the stretching of the C=O group of PLGA-PEG-PLGA copolymer while the low intensity peak at about 1450 cm^{-1} characterized C-O-C group and C-H bond of the methyl group. Another low intensity peak at 1180 cm^{-1} merging in the highest one was assigned to the ether group of the copolymer. The stretching of CH, CH_2, CH_3 groups of the PLGA-PEG-PLGA copolymer were attributed to the band at 2800-2900 cm^{-1} [63]. The highest peak of the spectrum at 1020 cm^{-1} was characteristic for the PO_4^{3-} ions of $Ca_3(PO_4)_2$, which is the major component of the CPC. The height of this peak indicates that the amount of this substance is the largest in the entire cement content. The next merging peak in the highest one was at 960 cm^{-1} and was attributed also to PO_4^{3-} ions. The low intensity peak around 870 cm^{-1} was observed for CO_3^{2-} groups of $CaCO_3$ [64][65]. The most sensitive spectral region for the protein secondary structural components are the bands at about 1600 cm^{-1} assigned to stretching of C=O group, which is characteristic for the peptide bond forming proteins. There was also observed frayed wide belt at 3300 cm^{-1} assigned to the stretching of NH group, which is also characteristic for the peptide bond [66]. However, this area could be also attributed to OH groups, when oxygen forms hydrogen bonds [63].

The amount of lysostaphin LYSSTAPH-S in the samples was much more lower compared to the amount of cement-forming ceramics. Due to the high intensity of the ceramic peaks, the others were very shady and small. The solution for the next time would be to choose only certain areas for the measurement (e.g. 3500-2500 cm^{-1}) and so create a better and clearer spectrum. The spectra of lysostaphin, lysozyme and albumin did not differ very much from each other. The only differences were in the intensity of the peaks.

6 CONCLUSION

In this work, we successfully prepared lysostaphin-loaded, self-setting and injectable calcium phosphate bone cement serving as a bone substitute and drug delivery system for possible treatment of osteomyelitis. The release experiment showed that there was released only about 3.26% of lysostaphin LYSSTAPH-S in 35 days. There were used model proteins lysozyme and albumin for the release experiment. The results showed that the release of these proteins was also quite poor. The high binding affinity between CPC and loaded protein has often proved to be a major problem in the release of higher amounts of proteins. It is considered whether higher amout of LYSSTAPH-S and model proteins would be released after the cement disintegrated in acidic conditions. The antibacterial activity assay showed that lysostaphin LYSSTAPH-S is effective against Gram-positive bacteria methicillin-resistant *Staphylococcus aureus*, which is resistant to almost all currently used antibiotics. ATR-FTIR measurement confirmed that the ingredients of the cements samples were PLGA-PEG-PLGA copolymer, but predominantly tricalcium phosphate. Signals corresponding to peptide bonds of the enzyme were also detected in the LYSSTAPH-S-loaded CPC sample, but these peaks were very low in intensity due to the predominant peaks of the ceramic phase. This new and original lysostaphin-loaded CPC has potential for the application as a replacement of bone and drug delivery system, but some of the used methods must be improved and studied in more depth to better understand the protein-calcium phosphate interactions.

7 REFERENCES

[1] CLARKE, Bart. Normal Bone Anatomy and Physiology. *Clinical Journal of the American Society of Nephrology* [online]. 2008, **3**(Supplement 3), S131-S139 [cit. 2020-02-11]. DOI: 10.2215/CJN.04151206. ISSN 1555-9041. Available from: http://cjasn.asnjournals.org/lookup/doi/10.2215/CJN.04151206

[2] XUE, Bai, Cheng ZHANG, Yihan WANG, et al. A Novel Controlled-Release System for Antibacterial Enzyme Lysostaphin Delivery Using Hydroxyapatite/Chitosan Composite Bone Cement. *PLoS ONE* [online]. 2014, 9(12) [cit. 2020-07-11]. DOI: 10.1371/journal.pone.0113797. ISSN 1932-6203. Available from: https://dx.plos.org/10.1371/journal.pone.0113797

[3] SNODDY, Brian, Ambalangodage C. JAYASURIYA, Yihan WANG, et al. The use of nanomaterials to treat bone infections. *Materials Science and Engineering: C* [online]. 2016, 67(12), 822-833 [cit. 2020-07-11]. DOI: 10.1016/j.msec.2016.04.062. ISSN 09284931. Available from: https://linkinghub.elsevier.com/retrieve/pii/S0928493116303691

[4] FATHI, M., A. KHOLTEI, S. EL YOUBI, et al. Setting Properties of Calcium Phosphate Bone Cement: Structural and spectroscopic characterization. *Materials Today: Proceedings* [online]. 2019, 13(4), 876-881 [cit. 2020-01-28]. DOI: 10.1016/j.matpr.2019.04.051. ISSN 22147853. Available from: https://linkinghub.elsevier.com/retrieve/pii/S2214785319306431

[5] WEKWEJT, M., N. MORITZ, B. ŚWIECZKO-ŻUREK, et al. Biomechanical testing of bioactive bone cements – a comparison of the impact of modifiers: antibiotics and nanometals. *Polymer Testing* [online]. 2018, **70**(1), 234-243 [cit. 2020-01-28]. DOI: 10.1016/j.polymertesting.2018.07.014. ISSN 01429418. Available from: https://linkinghub.elsevier.com/retrieve/pii/S014294181830498

[6] BASTOS, Maria do Carmo de Freire, Bruna Gonçalves COUTINHO a Marcus Lívio Varella COELHO. Lysostaphin: A Staphylococcal Bacteriolysin with Potential Clinical Applications. *Pharmaceuticals* [online]. 2010, 3(4), 1139-1161 [cit. 2019-12-04]. DOI: 10.3390/ph3041139. ISSN 1424-8247. Available from: http://www.mdpi.com/1424-8247/3/4/1139

[7] FLORENCIO-SILVA, Rinaldo, Gisela Rodrigues da Silva SASSO, Estela SASSO-CERRI, Manuel Jesus SIMÕES a Paulo Sérgio CERRI. Biology of Bone Tissue: Structure, Function, and Factors That Influence Bone Cells. *BioMed Research International* [online]. 2015, 2015(Supplement 3), 1-17 [cit. 2020-02-11]. DOI: 10.1155/2015/421746. ISSN 2314-6133. Available from: http://www.hindawi.com/journals/bmri/2015/421746/

[8] RALSTON, Stuart H., Gisela Rodrigues da Silva SASSO, Estela SASSO-CERRI, Manuel Jesus SIMÕES a Paulo Sérgio CERRI. Bone structure and metabolism: Structure, Function, and Factors That Influence Bone Cells. *Medicine* [online]. 2013, 41(10), 581-585 [cit. 2020-02-11]. DOI: 10.1016/j.mpmed.2013.07.007. ISSN 13573039. Available from: https://linkinghub.elsevier.com/retrieve/pii/S1357303913002120

[9] LOPÉZ LANDA, Alejandro. In: *Matmatch* [online]. 2019, 5.9.2019 [cit. 2020-02-11]. Available from: https://matmatch.com/blog/synthetic-calcium-phosphates-the-man-made-bone/

[10] BEJON, Philip a Esther ROBINSON. Bone and joint infection. *Medicine* [online]. 2013, 41(12), 719-722 [cit. 2020-02-15]. DOI: 10.1016/j.mpmed.2013.09.008. ISSN 13573039. Available from: https://linkinghub.elsevier.com/retrieve/pii/S1357303913002703

[11] SIGMUND, Irene K. a Martin A. MCNALLY. Diagnosis of bone and joint infections. *Orthopaedics and Trauma* [online]. 2019, **33**(3), 144-152 [cit. 2020-02-15]. DOI: 10.1016/j.mporth.2019.03.001. ISSN 18771327. Available from: https://linkinghub.elsevier.com/retrieve/pii/S1877132719300259

[12] LI, Hui, Shutao ZHANG, Shicheng HUO, Haozheng TANG, Bin'en NIE, Xinhua QU a Bing YUE. Effects of staphylococcal infection and aseptic inflammation on bone mass and biomechanical properties in a rabbit model. *Journal of Orthopaedic Translation* [online]. 2019, 33(3), 144-152 [cit. 2020-02-15]. DOI: 10.1016/j.jot.2019.11.006. ISSN 2214031X. Available from: https://linkinghub.elsevier.com/retrieve/pii/S2214031X19302451

[13] KHURANA A, CHHAWRA S, GUPTA R, KUMAR S. Osteomyelitis of Fibula Rare Case with Various Differential Diagnosis. *J Orthop Case Rep*. 2017;7(3):59-62 [cit. 2020-12-07]. DOI:10.13107/jocr.2250-0685.806. Available from: https://pubmed.ncbi.nlm.nih.gov/29051882/

[14] GATADI, Srikanth, Y.V. MADHAVI, Sidharth CHOPRA a Srinivas NANDURI. Promising antibacterial agents against multidrug resistant Staphylococcus aureus: A Staphylococcal Bacteriolysin with Potential Clinical Applications. *Bioorganic Chemistry* [online]. 2019, 92(4), 1139-1161 [cit. 2019-12-04]. DOI: 10.1016/j.bioorg.2019.103252. ISSN 00452068. Available from: https://linkinghub.elsevier.com/retrieve/pii/S0045206819302238

[15] CONG, Yanguang, Sijin YANG, Xiancai RAO a Srinivas NANDURI. Vancomycin resistant Staphylococcus aureus infections: A review of case updating and clinical features. *Journal of Advanced Research* [online]. 2020, 21(4), 169-176 [cit. 2019-12-04]. DOI: 10.1016/j.jare.2019.10.005. ISSN 20901232. Available from: https://linkinghub.elsevier.com/retrieve/pii/S2090123219301638

[16] SOARES, Geisla Mary Silva, Luciene Cristina FIGUEIREDO, Marcelo FAVERI, Sheila Cavalca CORTELLI, Poliana Mendes DUARTE a Magda FERES. Mechanisms of action of systemic antibiotics used in periodontal treatment and mechanisms of bacterial resistance to these drugs. *Journal of Applied Oral Science* [online]. 2012, **20**(3), 295-309 [cit. 2020-03-22]. DOI: 10.1590/S1678-77572012000300002. ISSN 1678-7757. Available from: https://dx.plos.org/10.1371/journal.ppat.0030102

[17] KAPOOR, Garima, Saurabh SAIGAL a Ashok ELONGAVAN. Action and resistance mechanisms of antibiotics: A guide for clinicians. *Journal of Anaesthesiology Clinical Pharmacology* [online]. 2017, 33(3) [cit. 2020-07-11]. DOI: 10.4103/joacp.JOACP_349_15. ISSN 0970-9185. Available from: http://www.joacp.org/text.asp?2017/33/3/300/214313

[18] INZANA, Jason A., Edward M. SCHWARZ, Stephen L. KATES a Hani A. AWAD. Biomaterials approaches to treating implant-associated osteomyelitis. *Biomaterials* [online]. 2016, 81, 58-71 [cit. 2020-07-11]. DOI: 10.1016/j.biomaterials.2015.12.012. ISSN 01429612. Available from: https://linkinghub.elsevier.com/retrieve/pii/S0142961215009941

[19] SPELLBERG, B., B. A. LIPSKY, Stephen L. KATES a Hani A. AWAD. Systemic Antibiotic Therapy for Chronic Osteomyelitis in Adults: A guide for clinicians. *Clinical Infectious Diseases* [online]. 2012, 54(3), 393-407 [cit. 2020-07-11]. DOI: 10.1093/cid/cir842. ISSN 1058-4838. Available from: https://academic.oup.com/cid/article-lookup/doi/10.1093/cid/cir842

[20] CHARNLEY, John. ANCHORAGE OF THE FEMORAL HEAD PROSTHESIS TO THE SHAFT OF THE FEMUR. *The Journal of Bone and Joint Surgery. British volume* [online]. 1960, 42-B(1), 28-30 [cit. 2020-07-12]. DOI: 10.1302/0301-620X.42B1.28. ISSN 0301-620X. Available from: http://online.boneandjoint.org.uk/doi/10.1302/0301-620X.42B1.28

[21] KENNY, S. M. a M. BUGGY. ANCHORAGE OF THE FEMORAL HEAD PROSTHESIS TO THE SHAFT OF THE FEMUR. *Journal of Materials Science: Materials in Medicine* [online]. 1960, 14(11), 923-938 [cit. 2020-07-12]. DOI: 10.1023/A:1026394530192. ISSN 09574530. Available from: http://link.springer.com/10.1023/A:1026394530192

[22] VAISHYA, Raju, Mayank CHAUHAN a Abhishek VAISH. Bone cement. *Journal of Clinical Orthopaedics and Trauma* [online]. 2013, 4(4), 157-163 [cit. 2020-07-11]. DOI: 10.1016/j.jcot.2013.11.005. ISSN 09765662. Available from: https://linkinghub.elsevier.com/retrieve/pii/S0976566213001057

[23] YOUSEFI, Azizeh-Mitra. *A review of calcium phosphate cements and acrylic bone cements as injectable materials for bone repair and implant fixation* [online]. 2019, **17**(4) [cit. 2020-07-11]. DOI: 10.1177/2280800019872594. ISSN 2280-8000. Available from: http://journals.sagepub.com/doi/10.1177/2280800019872594

[24] ARORA, Manit, Mayank CHAUHAN a Abhishek VAISH. Polymethylmethacrylate bone cements and additives: A review of the literature. *World Journal of Orthopedics* [online]. 2013, 4(2), 157-163 [cit. 2020-07-11]. DOI: 10.5312/wjo.v4.i2.67. ISSN 2218-5836. Available from: http://www.wjgnet.com/2218-5836/full/v4/i2/67.htm

[25] AYRE, Wayne Nishio, James C. BIRCHALL, Samuel L. EVANS, Stephen P. DENYER, Deepa BOSE a M. A. MCNALLY. A novel liposomal drug delivery system for PMMA bone cements: a review of 21 patients in a regional trauma centre. *Journal of Biomedical Materials Research Part B: Applied Biomaterials* [online]. 2016, 104(8), 1510-1524 [cit. 2020-07-11]. DOI: 10.1002/jbm.b.33488. ISSN 15524973. Available from: http://doi.wiley.com/10.1002/jbm.b.33488

[26] BEUERLEIN, Murray J S, Michael D MCKEE, Stephen L. KATES a Hani A. AWAD. Calcium Sulfates: What Is the Evidence? *Journal of Orthopaedic Trauma* [online]. 2010, 24(3), S46-S51 [cit. 2020-07-11]. DOI: 10.1097/BOT.0b013e3181cec48e. ISSN 0890-5339. Available from: http://journals.lww.com/00005131-201003001-00010

[27] TAN H, YANG S, DAI P, LI W, YUE B. Preparation and physical characterization of calcium sulfate cement/silica-based mesoporous material composites for controlled release of BMP-2. *Int J Nanomedicine*. 2015; 10:4341-4350. Published 2015 Jul 7. [cit. 2020-07-11] DOI:10.2147/IJN.S85763. Available from: https://pubmed.ncbi.nlm.nih.gov/26185438/

[28] FERGUSON, J. Y., M. DUDAREVA, N. D. RILEY, D. STUBBS, B. L. ATKINS a M. A. MCNALLY. The use of a biodegradable antibiotic-loaded calcium sulphate carrier containing tobramycin for the treatment of chronic osteomyelitis: A review of the literature. *World Journal of Orthopedics* [online]. 2014, 96-B(6), 829-836 [cit. 2020-07-11]. DOI: 10.1302/0301-620X.96B6.32756. ISSN 2049-4394. Available from: http://online.boneandjoint.org.uk/doi/10.1302/0301-620X.96B6.32756

[29] HUMM, Gemma, Saqib NOOR, Philippa BRIDGEMAN, Michael DAVID, Deepa BOSE a M. A. MCNALLY. Adjuvant treatment of chronic osteomyelitis of the tibia following exogenous trauma using OSTEOSET®-T: a review of 21 patients in a regional trauma centre. *Strategies in Trauma and Limb Reconstruction* [online]. 2014, **9**(3), 157-161 [cit. 2020-07-11]. DOI: 10.1007/s11751-014-0206-y. ISSN 1828-8936. Available from: https://www.stlrjournal.com/doi/10.1007/s11751-014-0206-y

[30] VOJTOVA, Lucy, Lenka MICHLOVSKA, Kristyna VALOVA, et al. The Effect of the Thermosensitive Biodegradable PLGA–PEG–PLGA Copolymer on the Rheological, Structural and Mechanical Properties of Thixotropic Self-Hardening Tricalcium Phosphate Cement. International Journal of Molecular Sciences [online]. 2019, 20(2) [cit. 2020-01-28]. DOI: 10.3390/ijms20020391. ISSN 1422-0067. Available from: http://www.mdpi.com/1422-0067/20/2/391

[31] MORENO, Daniel, Fabio VARGAS, Jeisson RUIZ, et al. Solid-state synthesis of alpha tricalcium phosphate for cements used in biomedical applications: Structural and spectroscopic characterization. *Boletín de la Sociedad Española de Cerámica y Vidrio* [online]. 2019, 13(4), 876-881 [cit. 2020-01-28]. DOI: 10.1016/j.bsecv.2019.11.004. ISSN 03663175. Available from: https://linkinghub.elsevier.com/retrieve/pii/S0366317519300986

[32] GOTO, Takashi, Hirokazu KATSUI, Aneta ZIMA, et al. Chemical Vapor Deposition of Ca–P–O Film Coating: from ceramics to calcium phosphate cements. *Interface Oral Health Science 2014* [online]. Tokyo: Springer Japan, 2015, 2015-9-26, 31(4), 103-115 [cit. 2020-01-28]. DOI: 10.1007/978-4-431-55192-8_9. ISBN 978-4-431-55125-6. ISSN 00201383. Available from: http://link.springer.com/10.1007/978-4-431-55192-8_9

[33] BOHNER, M., Agnieszka KAFLAK, Aneta ZIMA, et al. Calcium orthophosphates in medicine: from ceramics to calcium phosphate cements. *Injury* [online]. 2000, 31(4), D37-D47 [cit. 2020-01-28]. DOI: 10.1016/S0020-1383(00)80022-4. ISSN 00201383. Available from: https://linkinghub.elsevier.com/retrieve/pii/S0020138300800224

[34] MEHDAWI, I.M., A. YOUNG, Aneta ZIMA, et al. Antibacterial composite restorative materials for dental applications: from ceramics to calcium phosphate cements. *Biomaterials and Medical Device-Associated Infections* [online]. Elsevier, 2015, 2015, 31(4), 199-221 [cit. 2020-01-28]. DOI: 10.1533/9780857097224.2.199. ISBN 9780857095978. ISSN 00201383. Available from: https://linkinghub.elsevier.com/retrieve/pii/B9780857095978500104

[35] KOLMAS, Joanna, Agnieszka KAFLAK, Aneta ZIMA, et al. Alpha-tricalcium phosphate synthesized by two different routes: Structural and spectroscopic characterization. *Ceramics International* [online]. 2015, 41(4), 5727-5733 [cit. 2020-01-28]. DOI: 10.1016/j.ceramint.2014.12.159. ISSN 02728842. Available from: https://linkinghub.elsevier.com/retrieve/pii/S0272884215000152

[36] SHI, Haishan, Wenqian ZHANG, Xu LIU, et al. Synergistic effects of citric acid-sodium alginate on physicochemical properties of α-tricalcium phosphate bone cement: Structural and spectroscopic characterization. *Ceramics International* [online]. 2019, 45(2), 2146-2152 [cit. 2020-01-28]. DOI: 10.1016/j.ceramint.2018.10.124. ISSN 02728842. Available from: https://linkinghub.elsevier.com/retrieve/pii/S0272884218329304

[37] XU, Hockin HK, Ping WANG, Lin WANG, et al. Calcium phosphate cements for bone engineering and their biological properties: Structural and spectroscopic characterization. *Bone Research* [online]. 2017, **5**(1), 2146-2152 [cit. 2020-01-28]. DOI: 10.1038/boneres.2017.56. ISSN 2095-6231. Available from: http://www.nature.com/articles/boneres201756

[38] LOZANO-CALDERÓN, Santiago, Michael MOORE, Matthew LIEBMAN, Jesse B. JUPITER, Deepa BOSE a M. A. MCNALLY. Distal Radius Osteotomy in the Elderly Patient Using Angular Stable Implants and Norian Bone Cement: a review of 21 patients in a regional trauma centre. *The Journal of Hand Surgery* [online]. 2007, **32**(7), 976-983 [cit. 2020-07-11]. DOI: 10.1016/j.jhsa.2007.05.005. ISSN 03635023. Available from: https://linkinghub.elsevier.com/retrieve/pii/S0363502307004947

[39] GINEBRA, M.P., T. TRAYKOVA, J.A. PLANELL, Jesse B. JUPITER, Deepa BOSE a M. A. MCNALLY. Calcium phosphate cements as bone drug delivery systems: A review. *Journal of Controlled Release* [online]. 2006, 113(2), 102-110 [cit. 2020-07-11]. DOI: 10.1016/j.jconrel.2006.04.007. ISSN 01683659. Available from: https://linkinghub.elsevier.com/retrieve/pii/S0168365906001775

[40] DYM, Harry a Joseph ZEIDAN. Microbiology of Acute and Chronic Osteomyelitis and Antibiotic Treatment. *Dental Clinics of North America* [online]. 2017, 61(2), 271-282 [cit. 2020-03-25]. DOI: 10.1016/j.cden.2016.12.001. ISSN 00118532. Available from: https://linkinghub.elsevier.com/retrieve/pii/S0011853216301355

[41] CHOO, Eun Ju, Henry F. CHAMBERS a Xiancai RAO. Treatment of Methicillin-Resistant Staphylococcus aureus Bacteremia: A review of case updating and clinical features. *Journal of Advanced Research* [online]. 2016, 48(4), 169-176 [cit. 2020-03-25]. DOI: 10.3947/ic.2016.48.4.267. ISSN 2093-2340. Available from: https://synapse.koreamed.org/DOIx.php?id=10.3947/ic.2016.48.4.267

[42] CHEN, Gaoyang, Bo LIU, He LIU, Hanyang ZHANG, Kerong YANG, Qingyu WANG, Jianxun DING a Fei CHANG. Calcium Phosphate Cement loaded with 10% vancomycin delivering high early and late local antibiotic concentration in vitro: A review. *Journal of Controlled Release* [online]. 2018, 104(8), 1271-1275 [cit. 2020-07-11]. DOI: 10.1016/j.otsr.2018.07.007. ISSN 18770568. Available from: https://linkinghub.elsevier.com/retrieve/pii/S1877056818302196

[43] HEGEROVA, Dagmar, Radek VESELY, Kristyna CIHALOVA, et al. Antimicrobial Agent Based on Selenium Nanoparticles and Carboxymethyl Cellulose for the Treatment of Bacterial Infections. *Journal of Biomedical Nanotechnology* [online]. 2017, 13(7), 767-777 [cit. 2020-03-26]. DOI: 10.1166/jbn.2017.2384. ISSN 1550-7033. Available from: https://www.ingentaconnect.com/content/10.1166/jbn.2017.2384

[44] WANG, Linlin, Chen HU, Longquan SHAO, et al. The antimicrobial activity of nanoparticles: present situation and prospects for the future. *International Journal of Nanomedicine* [online]. 2017, 12(7), 1227-1249 [cit. 2020-03-26]. DOI: 10.2147/IJN.S121956. ISSN 1178-2013. Available from: https://www.dovepress.com/the-antimicrobial-activity-of-nanoparticles-present-situation-and-pros-peer-reviewed-article-IJN

[45] SHAIKH, Sibhghatulla, Nazia NAZAM, Syed Mohd Danish RIZVI, Khurshid AHMAD, Mohammad Hassan BAIG, Eun Ju LEE, Inho CHOI a Fei CHANG. Mechanistic Insights into the Antimicrobial Actions of Metallic Nanoparticles and Their Implications for Multidrug Resistance: A review. *International Journal of Molecular Sciences* [online]. 2019, 20(10), 1271-1275 [cit. 2020-07-11]. DOI: 10.3390/ijms20102468. ISSN 1422-0067. Available from: https://www.mdpi.com/1422-0067/20/10/2468

[46] PAJOR, Kamil, Lukasz PAJCHEL, Barbara KOLODZIEJSKA, Joanna KOLMAS, Mohammad Hassan BAIG, Eun Ju LEE, Inho CHOI a Fei CHANG. Selenium-Doped Hydroxyapatite Nanocrystals–Synthesis, Physicochemical Properties and Biological Significance: A review. *Crystals* [online]. 2018, 8(5), 1271-1275 [cit. 2020-07-11]. DOI: 10.3390/cryst8050188. ISSN 2073-4352. Available from: http://www.mdpi.com/2073-4352/8/5/188

[47] KOLMAS, Joanna, Ewa GROSZYK, Dagmara KWIATKOWSKA-RÓŻYCKA, Joanna KOLMAS, Mohammad Hassan BAIG, Eun Ju LEE, Inho CHOI a Fei CHANG. Substituted Hydroxyapatites with Antibacterial Properties: A review. *BioMed Research International* [online]. 2014, 2014(5), 1-15 [cit. 2020-07-11]. DOI: 10.1155/2014/178123. ISSN 2314-6133. Available from: http://www.hindawi.com/journals/bmri/2014/178123/

[48] GRÉZLOVÁ, Veronika. Optimization of antibacterial properties of polymer-phosphate bone fillers [online]. Brno, 2018 [cit. 2020-12-7]. Available from: https://www.vutbr.cz/studenti/zav-prace/detail/. Diploma thesis. Brno Uviversity of Technology, Faculty of Chemistry. Supervisor Lucy Vojtová

[49] DOLEŽÍLKOVÁ, Ivana, Martina MACKOVÁ a Tomáš MACEK. Antimikrobiální peptidy: Vztah mezi jejich strukturou a antimikrobiální aktivitou, Chemické Listy. 2011, č.105, s. 346-355

[50] BAHAR, Ali a Dacheng REN. Antimicrobial Peptides. *Pharmaceuticals* [online]. 2013, 6(12), 1543-1575 [cit. 2020-02-20]. DOI: 10.3390/ph6121543. ISSN 1424-8247. Available from: http://www.mdpi.com/1424-8247/6/12/1543

[51] STALLMANN, H. P., Maria CAPUCCHIO, Elena BIASIBETTI, Enrica PESSIONE, Simona CIRRINCIONE, Leonardo GIRAUDO, Antonio CORONA a Franco DOSIO. Continuous-release or burst-release of the antimicrobial peptide human lactoferrin 1-11 (hLF1-11) from calcium phosphate bone substitutes: A review. *Journal of Antimicrobial Chemotherapy* [online]. 2003, 52(5), 853-855 [cit. 2020-07-11]. DOI: 10.1093/jac/dkg443. ISSN 1460-2091. Available from: https://academic.oup.com/jac/article-lookup/doi/10.1093/jac/dkg443

[52] BRUNI, Natascia, Maria CAPUCCHIO, Elena BIASIBETTI, Enrica PESSIONE, Simona CIRRINCIONE, Leonardo GIRAUDO, Antonio CORONA a Franco DOSIO. Antimicrobial Activity of Lactoferrin-Related Peptides and Applications in Human and Veterinary Medicine: A review. *Molecules* [online]. 2016, **21**(6), 1-15 [cit. 2020-07-11]. DOI: 10.3390/molecules21060752. ISSN 1420-3049. Available from: http://www.mdpi.com/1420-3049/21/6/752

[53] SHRIVASTAVA, Arpita, Neeraj SHRIVASTAVA a Pradeep Kumar SINGH. Enzymes in Pharmaceutical Industry. *Enzymes in Food Biotechnology* [online]. Elsevier, 2019, 2019, , 591-602 [cit. 2020-03-17]. DOI: 10.1016/B978-0-12-813280-7.00034-7. ISBN 9780128132807. Available from: https://linkinghub.elsevier.com/retrieve/pii/B9780128132807000347

[54] BAYAZIDI, Pashew, Hadi ALMASI, Asghar Khosrowshahi ASL, Enrica PESSIONE, Simona CIRRINCIONE, Leonardo GIRAUDO, Antonio CORONA a Franco DOSIO. Immobilization of lysozyme on bacterial cellulose nanofibers: Characteristics, antimicrobial activity and morphological properties. *International Journal of Biological Macromolecules* [online]. 2018, 107(5), 2544-2551 [cit. 2020-07-11]. DOI: 10.1016/j.ijbiomac.2017.10.137. ISSN 01418130. Available from: https://linkinghub.elsevier.com/retrieve/pii/S0141813017329823

[55] HERBERT, Silvia, Agnieszka BERA, Christiane NERZ, et al. Molecular Basis of Resistance to Muramidase and Cationic Antimicrobial Peptide Activity of Lysozyme in Staphylococci: Characteristics, antimicrobial activity and morphological properties. *PLoS Pathogens* [online]. 2007, 3(7), 2544-2551 [cit. 2020-07-11]. DOI: 10.1371/journal.ppat.0030102. ISSN 1553-7374. Available from: https://dx.plos.org/10.1371/journal.ppat.0030102

[56] STEWARD, Karen. Gram positive vs Gram negative. *Technology Networks* [online]. Technology Networks, 2019, 21.8.2019 [cit. 2020-07-12]. Available from: https://www.technologynetworks.com/immunology/articles/gram-positive-vs-gram-negative-323007

[57] MAK, Paweł, Neeraj SHRIVASTAVA a Pradeep Kumar SINGH. Staphylococcal Bacteriocins. *Pet-To-Man Travelling Staphylococci* [online]. Elsevier, 2018, 2018, , 161-171 [cit. 2020-03-17]. DOI: 10.1016/B978-0-12-813547-1.00013-3. ISBN 9780128135471. Available from: https://linkinghub.elsevier.com/retrieve/pii/B9780128135471000133

[58] WU, J. A., C. KUSUMA, J. J. MOND a J. F. KOKAI-KUN. Lysostaphin Disrupts Staphylococcus aureus and Staphylococcus epidermidis Biofilms on Artificial Surfaces: A Staphylococcal Bacteriolysin with Potential Clinical Applications. *Antimicrobial Agents and Chemotherapy* [online]. 2003, 47(11), 3407-3414 [cit. 2020-03-05]. DOI: 10.1128/AAC.47.11.3407-3414.2003. ISSN 0066-4804. Available from: http://aac.asm.org/cgi/doi/10.1128/AAC.47.11.3407-3414.2003

[59] YU, Lin, Jiandong DING, Xuezhi ZHUO, et al. Injectable hydrogels as unique biomedical materials. *Chemical Society Reviews* [online]. 2008, **37**(8), 1551-1565 [cit. 2020-02-06]. DOI: 10.1039/b713009k. ISSN 0306-0012. Available from: http://xlink.rsc.org/?DOI=b713009k

[60] WANG, Puxiu, Wei CHU, Xuezhi ZHUO, et al. Modified PLGA–PEG–PLGA thermosensitive hydrogels with suitable thermosensitivity and properties for use in a drug delivery system. *Journal of Materials Chemistry B* [online]. 2017, **5**(8), 1551-1565 [cit. 2020-02-06]. DOI: 10.1039/C6TB02158A. ISSN 2050-750X. Available from: http://xlink.rsc.org/?DOI=C6TB02158A

[61] MAEDA, Tomoki, James C. BIRCHALL, Samuel L. EVANS, Stephen P. DENYER, Deepa BOSE a M. A. MCNALLY. Structures and Applications of Thermoresponsive Hydrogels and Nanocomposite-Hydrogels Based on Copolymers with Poly (Ethylene Glycol) and Poly (Lactide-Co-Glycolide) Blocks: a review of 21 patients in a regional trauma centre. *Bioengineering* [online]. 2019, 6(4), 1510-1524 [cit. 2020-07-11]. DOI: 10.3390/bioengineering6040107. ISSN 2306-5354. Available from: https://www.mdpi.com/2306-5354/6/4/107

[62] LYSÁKOVÁ, Klára. Optimization of methods for protein analysis released from *thermosensitive hydrogel* [online]. Brno, 2019 [cit. 2019-05.06]. Available from: https://www.vutbr.cz/studenti/zav-prace/detail/117344. Diploma thesis. Brno Uviversity of Technology, Faculty of Chemistry. Supervisor Lucy Vojtová

[63] PEREIRA, Emiliane Daher, Renata CERRUTI, Edson FERNANDES, et al. Influence of PLGA and PLGA-PEG on the dissolution profile of oxaliplatin. *Polímeros* [online]. 2016, **26**(2), 137-143 [cit. 2020-07-14]. DOI: 10.1590/0104-1428.2323. ISSN 1678-5169.

[64] SALMA, Kristine, N. BORODAJENKO, A. PLATA, et al. Fourier Transform Infrared Spectra of Technologically Modified Calcium Phosphates. *14th Nordic-Baltic Conference on Biomedical Engineering and Medical Physics* [online]. Berlin, Heidelberg: Springer Berlin Heidelberg, 2008, 2008, **26**(2), 68-71 [cit. 2020-07-14]. IFMBE Proceedings. DOI: 10.1007/978-3-540-69367-3_19. ISBN 978-3-540-69366-6. ISSN 1678-5169. Available from: http://link.springer.com/10.1007/978-3-540-69367-3_19

[65] LIU, Zongguang, Shuxin QU, Xiaotong ZHENG, et al. Effect of polydopamine on the biomimetic mineralization of mussel-inspired calcium phosphate cement in vitro. *Materials Science and Engineering: C* [online]. Berlin, Heidelberg: Springer Berlin Heidelberg, 2014, 2008, 44(2), 44-51 [cit. 2020-07-14]. IFMBE Proceedings. DOI: 10.1016/j.msec.2014.07.063. ISBN 978-3-540-69366-6. ISSN 09284931. Available from: https://linkinghub.elsevier.com/retrieve/pii/S0928493114004810

[66] KONG, Jilie, Shaoning YU, Xiaotong ZHENG, et al. Fourier Transform Infrared Spectroscopic Analysis of Protein Secondary Structures. *Acta Biochimica et Biophysica Sinica* [online]. Berlin, Heidelberg: Springer Berlin Heidelberg, 2007, 2008, 39(8), 549-559 [cit. 2020-07-14]. IFMBE Proceedings. DOI: 10.1111/j.1745-7270.2007.00320.x. ISBN 978-3-540-69366-6. ISSN 1672-9145. Dostupné z: https://academic.oup.com/abbs/article-lookup/doi/10.1111/j.1745-7270.2007.00320.x

8 LIST OF TABLES

9 LIST OF FIGURES

10 LIST OF ABBREVIATIONS AND SYMBOLS

CoPS	Coagulase-positive
RNA	Ribonucleic acid
DNA	Deoxyribonucleic acid
CDHA	Calcium deficient hydroxyapatite
α, β, α’ -TCP	α, β, α’ -Tricalcium phosphate
CPC	Calcium phosphate cement
VISA	Vancomycin-intermediate *Staphylococcus aureus*
VRSA	Vancomycin-resistant *Staphylococcus aureus*
VSSA	Vancomycin-susceptible *Staphylococcus aureus*
PMMA	Poly(methyl methacrylate)
AgNPs	Silver nanoparticles
SeNPs	Selenium nanoparticles
Gly	Glycin
PEG	Polyethylen glycol
PLGA	Poly(lactic-co-glycolic acid)
UV-VIS	UltraViolet-Visible spectroscopy
ATR-FTIR	Attenuated total reflectance Fourier-transform infrared spectroscopy
AMPs	Antimicrobial peptides
MRSA	Methicillin-resistant *Staphylococcus aureus*
SA	*Staphylococcus aureus*
EC	*Escherichia coli*
MH medium	Mueller-Hinton medium